Foodborne Origin and Local and Global Spread of *Staphylococcus saprophyticus* Causing Human Urinary Tract Infections

Opeyemi U. Lawal, Maria J. Fraqueza, Ons Bouchami, Peder Worning, Mette D. Bartels, Maria L. Gonçalves, Paulo Paixão, Elsa Gonçalves, Cristina Toscano, Joanna Empel, Małgorzata Urbaś, M. Angeles Domínguez, Henrik Westh, Hermínia de Lencastre, Maria Miragaia

Staphylococcus saprophyticus is a primary cause of community-acquired urinary tract infections (UTIs) in young women. *S. saprophyticus* colonizes humans and animals but basic features of its molecular epidemiology are undetermined. We conducted a phylogenomic analysis of 321 *S. saprophyticus* isolates collected from human UTIs worldwide during 1997–2017 and 232 isolates from human UTIs and the pig-processing chain in a confined region during 2016–2017. We found epidemiologic and genomic evidence that the meat-production chain is a major source of *S. saprophyticus* causing human UTIs; human microbiota is another possible origin. Pathogenic *S. saprophyticus* belonged to 2 lineages with distinctive generic features that are globally and locally disseminated. Pangenome-wide approaches identified a strong association between pathogenicity and antimicrobial resistance, phages, platelet binding proteins, and an increased recombination rate. Our study provides insight into the origin, transmission, and population structure of pathogenic *S. saprophyticus* and identifies putative new virulence factors.

Staphylococcus saprophyticus is the cause of uncomplicated urinary tract infection (UTI) in 10%–20% of young women (*1*). Despite a greater successful treatment rate, *S. saprophyticus* UTI has a higher recurrent infection frequency than *Escherichia coli* UTI (*2*). Rare complications of *S. saprophyticus* UTI include acute pyelonephritis, nephrolithiasis, and endocarditis (*3*).

S. saprophyticus frequently colonizes humans and can be found in the gastrointestinal tract, vagina, and perineum (*4*). *S. saprophyticus* also is part of the gut and rectal flora of livestock, including pigs and cattle, and a frequent contaminant of meat and fermented food products (*1*). *S. saprophyticus* also has been recovered from polluted aquatic environments (*5*).

The reservoirs of *S. saprophyticus* causing UTI in humans are believed to be endogenous, but evidence is lacking. Moreover, given the frequent bacterial contamination of meat through the meat-processing chain, meat and food are speculated to be sources of human gut colonization and human *S. saprophyticus* infection (*6*). Some studies have reported high genetic diversity among isolates from human infections, food products, and other sources (*5*,*7*,*8*). However, previous studies were performed with a limited number of isolates, which prevented the description of the global and local molecular epidemiology of *S. saprophyticus*.

We used phenotypic, genomic, and pangenome-wide association study (pan-GWAS) approaches to characterize *S. saprophyticus* both globally and locally. In addition, we identified adaptive features that drive *S. saprophyticus* evolution, defined the *S. saprophyticus* population structure, investigated dissemination routes, and identified new pathogenicity factors.

Methods

Ethics Considerations

The human isolates used in our study were recovered as part of routine clinical diagnostic testing; thus,

Author affiliations: Universidade Nova de Lisboa, Oeiras, Portugal (O.U. Lawal, O. Bouchami, H. de Lencastre, M. Miragaia); Centre for Interdisciplinary Research in Animal Health (CIISA), Universidade de Lisboa, Lisbon, Portugal (M.J., Fraqueza); Hvidovre University Hospital, Hvidovre, Denmark (P. Worning, M.D. Bartels, H. Westh); SAMS Hospital, Lisbon (M.L. Gonçalves); Hospital da Luz, Lisbon (P. Paixão); Hospital Egas Moniz, Lisbon (E. Gonçalves, C. Toscano); Narodowy Instytut Leków, Warsaw, Poland (J. Empel, M. Urbaś); Hospital Universitari de Bellvitge, Barcelona, Spain (M.A. Domínguez); University of Copenhagen, Copenhagen, Denmark (H. Westh); The Rockefeller University, New York, New York, USA (H. de Lencastre)

DOI: https://doi.org/10.3201/eid2703.200852

ethics approval and informed consent were not required. All data were handled anonymously. Sample collection was in accordance with the European Parliament and Council decision for the epidemiologic surveillance and control of communicable disease through the European Antimicrobial Resistance Surveillance Network (http://www.ecdc.europa.eu/en/activities/surveillance/EARS-Net/Pages/index.aspx). Slaughterhouse samples were part of the routine control practices for evaluation of good hygiene practices and programs to assure meat safety (European Parliament and Council regulation no. 853/2004).

Bacterial Isolates

The global *S. saprophyticus* collection we used included 299 isolates from humans collected in 7 countries during 1997–2017: 286 from UTIs, 12 from invasive disease, and 1 from colonization (Appendix 1 Table 1, https://wwwnc.cdc.gov/EID/article/27/3/20-0852-App1.xlsx). We also analyzed the genomes of *S. saprophyticus* for 38 isolates from 5 other countries: 35 isolates from human UTIs (*8*), 2 from human hand swabs (*8*), an isolate from Byzantine Troy (*8*), and ATCC 15305 (*9*), a previously investigated human UTI-causing isolate.

The local collection included isolates collected in Lisbon, Portugal, during 2016–2017: 128 human UTI isolates collected in 3 hospitals and 104 slaughterhouse isolates collected from equipment, pork samples, workers' hands, and a pig's rectum. In addition, we included 5 isolates from animals and 12 isolates from food used in other studies (*8*) (Appendix 2, https://wwwnc.cdc.gov/EID/article/27/3/20-0852-App2.pdf).

Whole-Genome Sequencing and Assembly

Phylogenetic Analysis

We performed whole-genome sequencing (WGS) on MiSeq (Illumina, https://www.illumina.com) and MinIon nanopore (Oxford Nanopore, https://nanoporetech.com) platforms, as described (*10*) (Appendix 2). We separately analyzed global population and local epidemiology of *S. saprophyticus* and their phylogeny by using single-nucleotide polymorphisms (SNPs). We identified SNPs by mapping the draft genomes to a reference genome, *S. saprophyticus* ATCC 15305 (GenBank accession no. AP008934.1) by using the web-based CSI phylogeny version 1.4 (*11*) with the default parameter, but we disabled the minimum distance between SNPs in the parameter. We used Gubbins version 2.3.4 (*12*) with default parameters to concatenate SNPs and remove recombination regions. We reconstructed the phylogenies by using RAxML version 8.2.4 (https://github.com/stamatak/standard-RAxML) and generalized time-reversible nucleotide substitution with gamma correction model with 100 bootstrap value. We visualized the maximum-likelihood trees by using Interactive Tree of Life (ihttps://itol.embl.de) (Figures 1–3; Appendix 2 Figure 3). Recombination to mutation (r/m) ratios detected by using Gubbins were calculated as the average r/m of isolates in the entire collection and separately for each lineage by using as reference closed genomes of KS40 for lineage G and KS160 for lineage S, both obtained on the MinIon platform (Oxford Nanopore).

Pan-GWAS

We used Prokka version 1.13 (https://vicbioinformatics.com/software.prokka.shtml) to annotate genomes and defined the pangenome by using 85% blastp (https://blast.ncbi.nlm.nih.gov/Blast.cgi) identity in Roary version 3.12 (http://sanger-pathogens.github.io/Roary). We performed GWAS by using Scoary version 1.6.16 (*13*) to identify genes associated with lineages and considered Bonferroni corrected $p<0.05$ (odds ratio [OR] >1) statistically significant; we identified genes associated with epidemiologic groups and considered Benjamini Hochberg corrected and pairwise comparison $p<0.05$ statistically significant. Sequence data from this study are available in GenBank (accession no. PRJNA604222).

Resistome and Virulome Analyses

We screened genomes for resistance and virulence genes by using ResFinder version 2.3 (http://cge.cbs.dtu.dk/services/ResFinder), an in-house virulence genes database, and the virulence factor database (*14*), integrated into ABRicate version 0.5 (https://github.com/tseemann/abricate). We considered genes with a threshold $\geq$90% nucleotide identity and $\geq$60% coverage to be present.

Statistical Analyses

We used Prism 6.0 (GraphPad, https://www.graphpad.com) to compare the means of 2 groups. We used a 2-tailed unpaired Mann-Whitney test or χ^2 test for comparison and considered $p<0.05$ statistically significant.

Results

Lineages of *S. saprophyticus* Causing UTIs

Among study isolates, we first analyzed the diversity of *S. saprophyticus* causing UTIs by using genomic data of 321 human UTI isolates collected from 8 countries

on 4 continents during 1997–2017. From the SNPs initially detected, 42% arose from recombination events in the population, corresponding to a mean genome-wide r/m of 1.5:1, meaning that high accumulation of SNPs was due to recombination rather than mutation in UTI strains. The maximum-likelihood tree constructed from the 9,134 SNPs without recombination defined 2 lineages, which we called G and S (Figure 1). Most (74%, 236/321) UTI isolates were from lineage G and differed by 0–4,318 SNPs with an average nucleotide identity (ANI) of 98.5%–99.999%, whereas S isolates (26%, n = 85/321) were slightly less distantly

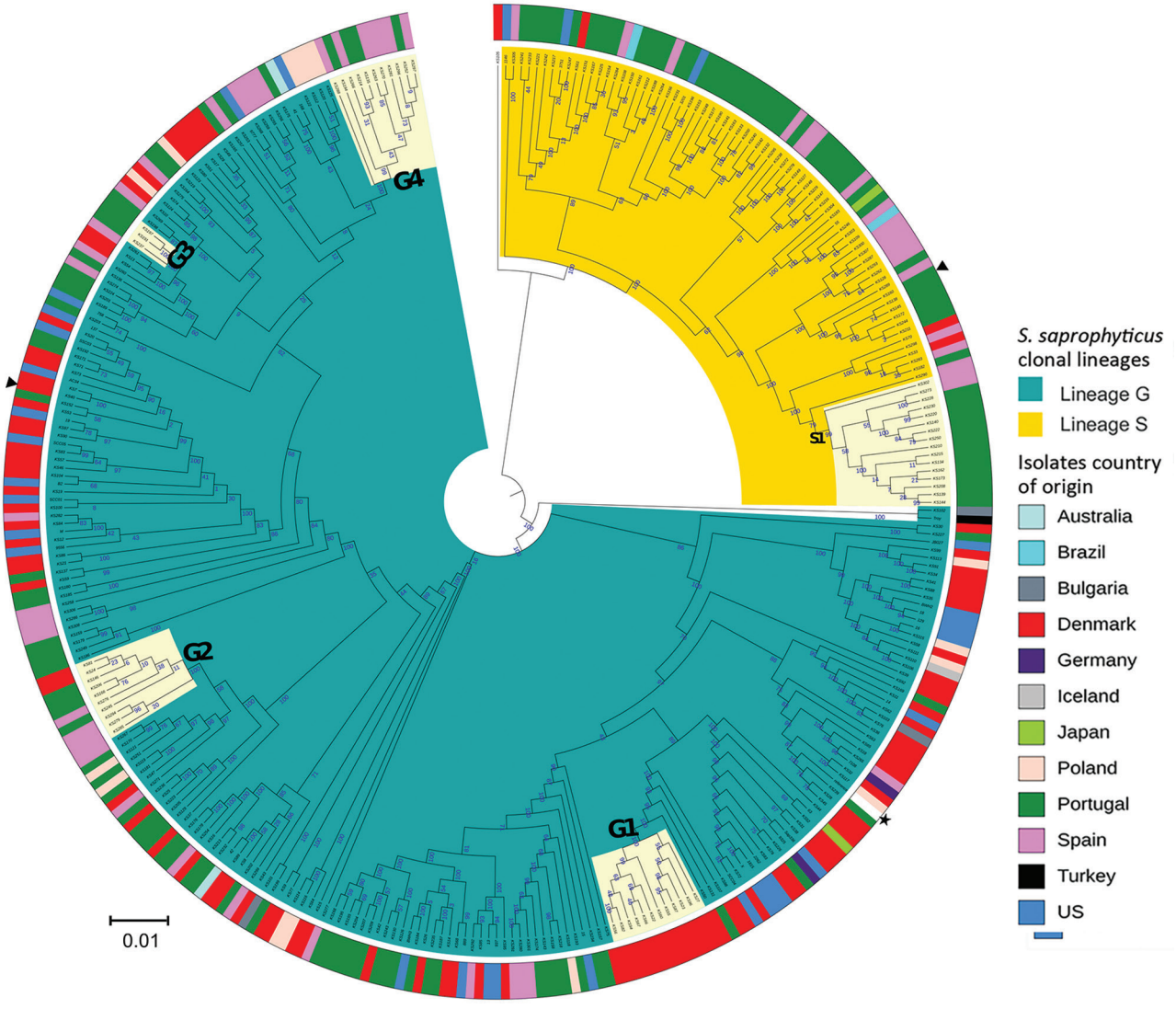

Figure 1. Maximum-likelihood tree of *Staphylococcus saprophyticus* isolates recovered from human infections and colonization globally, 1997–2017. The tree was constructed by using 9,134 SNPs without recombination. Among analyzed isolates, 321 were recovered from UTIs, 12 from blood, and 4 from colonization. Each node represents a strain; nodes with identical color belong to the same lineage. The assembled contigs were mapped to the reference genome *S. saprophyticus* ATCC 15305 (GenBank accession no. AP008934.1; black star). Polymorphic sites resulting from recombination events in the single-nucleotide polymorphism (SNP) alignments were filtered out by using Gubbins version 2.3.4 (*12*). Maximum likelihood tree was reconstructed by using RAxML version 8.2.4 (https://github.com/stamatak/standard-RAxML). We performed generalized time-reversible nucleotide substitution model with gamma correction with 100 bootstraps random resampling for support. We visualized the tree by using Interactive Tree of Life (iTOL; https://itol.embl.de). Black triangles represent isolates fully sequenced by using the long-read nanopore technologies and used as reference to estimate r/m in the respective lineage. Cream color represents clusters G1, G2, G3, G4, and S1, which had dissemination and transmission in same country and in different countries. The outer ring represents isolates' country of origin; blocks with identical color represent isolates from the same country. Of note, cluster G4 contains a pair of isolates collected in 2016 that had only 10 SNPs difference; one is a blood isolate from Barcelona, Spain (KS266) and the other is a UTI isolate recovered in Lisbon, Portugal (KS135). Scale bar indicates number of substitutions per site. UTI, urinary tract infection; r/m, recombination to mutation ratio.

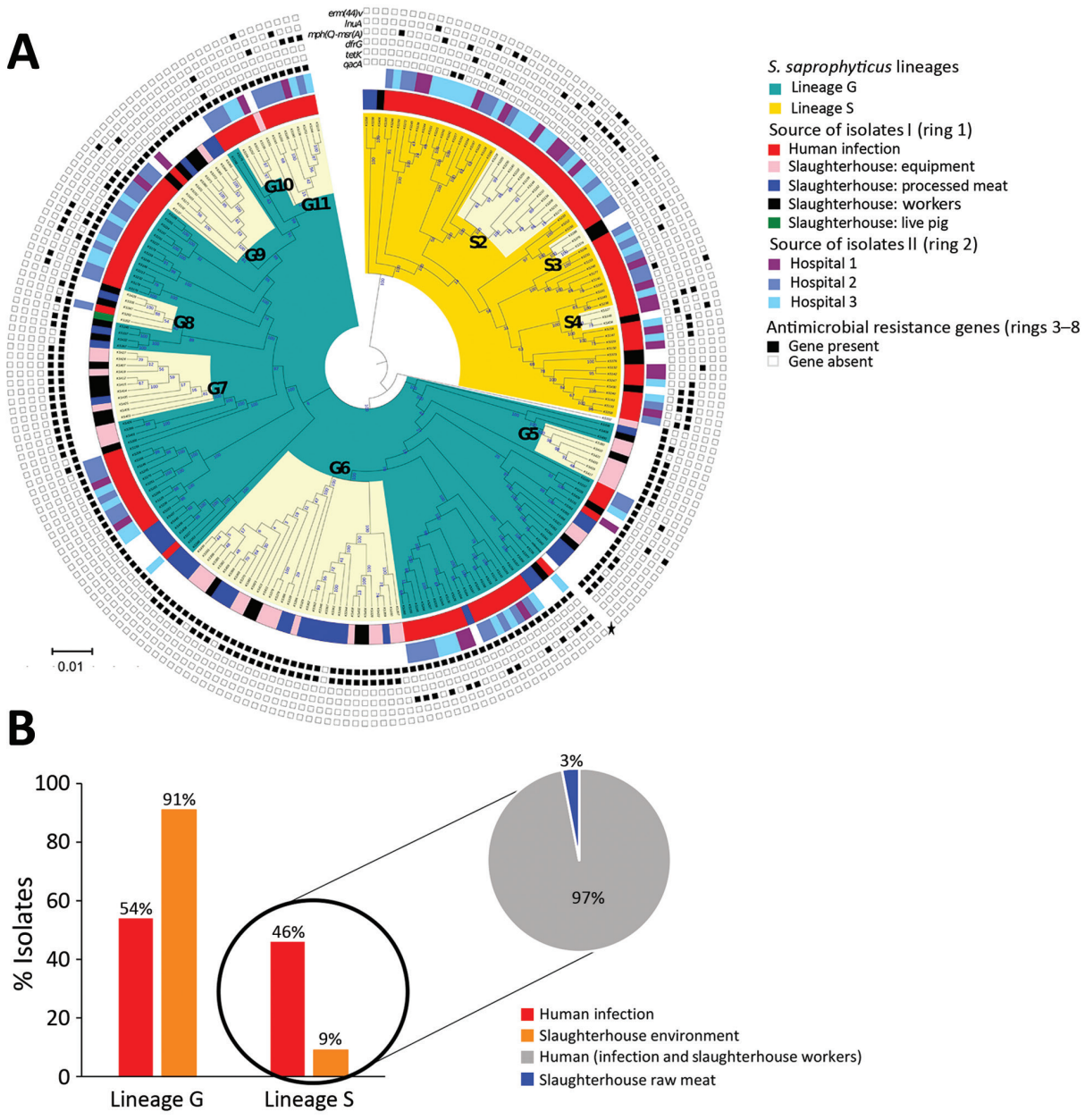

Figure 2. Phylogenomic analysis and distribution of *Staphylococcus saprophyticus* isolates collected from human infections and a slaughterhouse, Portugal, 2016–2017. A) Maximum-likelihood tree of 232 isolates from human infections or slaughterhouse contamination. The tree was constructed by using 14,110 single-nucleotide polymorphisms (SNPs) without recombination. Each node represents a strain; nodes with identical color belong to the same lineage. The assembled contigs were mapped to the reference genome *S. saprophyticus* ATCC 15305 (GenBank accession no. AP008934.1; black star). SNPs generated from each genome were concatenated to single alignment corresponding to position of the reference genome. Polymorphic sites resulting from recombination events in the SNP alignments were filtered out by using out by using Gubbins version 2.3.4 (*12*). Tree was reconstructed by using RAxML version 8.2.4 (https://github.com/stamatak/standard-RAxML). The generalized time-reversible nucleotide substitution model with gamma correction was performed with 100 bootstrap random re-samplings for support. The tree was visualized by using Interactive Tree of Life (iTOL; https://itol.embl.de). The clusters highlighted in cream represent admixture of isolates recovered from different sources that are closely related by SNPs in clusters G5–G11 and S2–S4. The inner ring (ring 1) represents genetic relatedness of isolates recovered from different sites inside the slaughterhouses and those recovered from infection in the community. The center ring (ring 2) identifies the isolates recovered from different hospitals. The outer rings (rings 3–8) represent the distribution of 6 genes that convey antimicrobial resistance. Scale bar indicates nucleotide substitutions per site. B) Source-based distribution of *S. saprophyticus* isolates in the lineage G and lineage S. Lineage G consisted isolates from infections, colonization, and contamination. Almost all (97%) isolates in lineage S are from human colonization and infection.

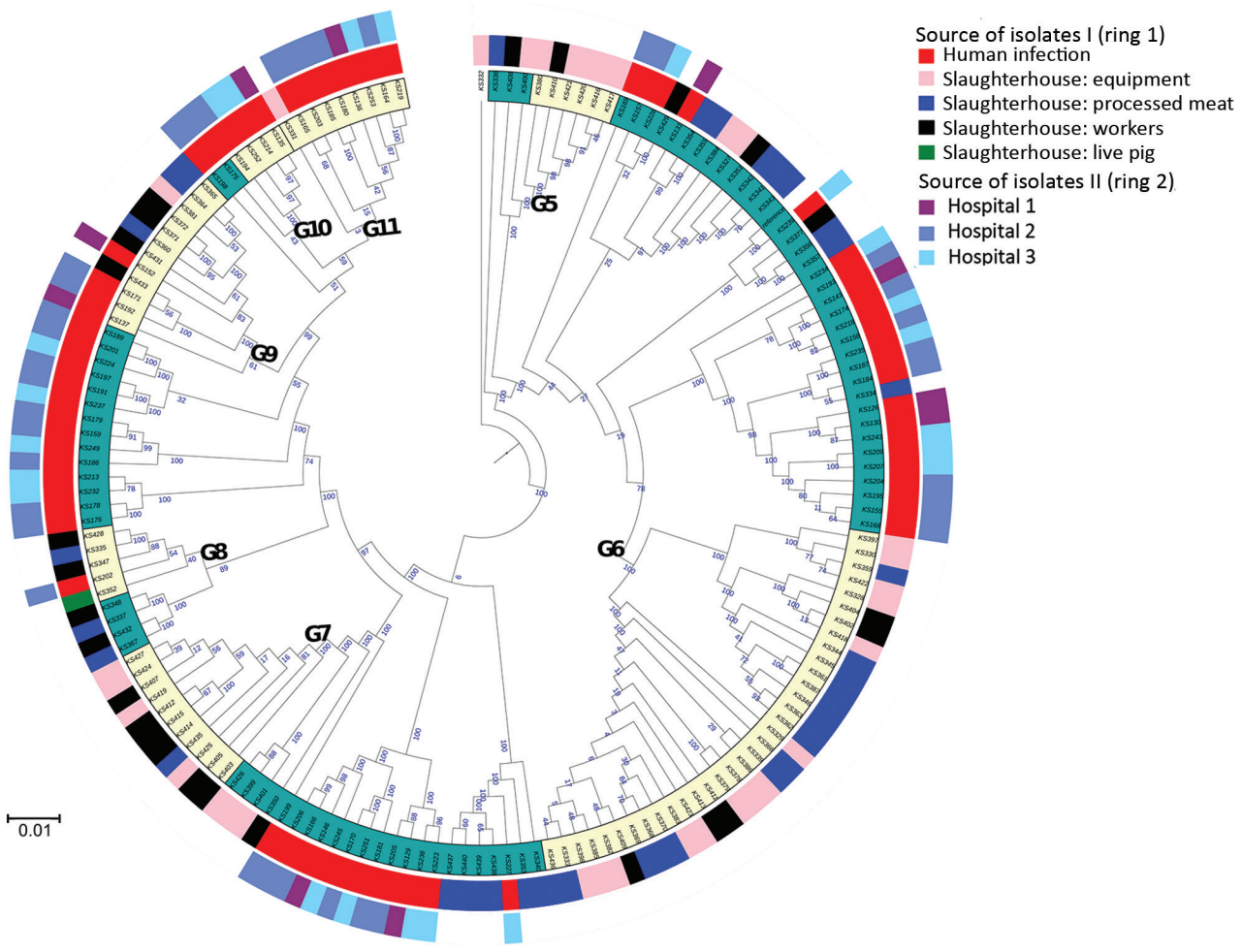

Figure 3. Maximum-likelihood tree depicting the genetic relatedness of *Staphylococcus saprophyticus* isolates belonging to clonal lineage G recovered from human infections or slaughterhouse contamination, Portugal, 2016–2017. Each node represents a strain. The tree was visualized by using Interactive Tree of Life (iTOL; https://itol.embl.de). Clusters highlighted in cream in the innermost ring represent admixture of isolates in clusters G5–G11, which were recovered from different sources and are closely related by single-nucleotide polymorphism. Ring 1 represents genetic relatedness of isolates recovered from different sites in the slaughterhouses and those recovered from infection in the community. Ring 2 depicts the isolates recovered from different hospitals. Scale bar indicates nucleotide substitutions per site.

related, differing by 0–3,540 SNPs with an ANI of 99.3%–99.991% (Appendix 2 Figure 1).

S. saprophyticus lineages we identified among UTI isolates worldwide had distinctive features indicative of 2 evolutionary histories. Although strains of both lineages had similar genome size as determined by their closed genomes (lineage G was 2.5 Mb and S 2.6 Mb), isolates from lineage S (n = 6) grew significantly faster in tryptic soy broth incubated at 37°C ($\mu_{average}$ = 0.34 h^{-1}) than G strains (n = 8) ($\mu_{average}$ = 0.22 h^{-1}; p = 0.0007) (Figure 4; Appendix 2). Moreover, we separately analyzed r/m of both lineages by using the respective closed genome of strains from each lineage as a reference and found that the mean estimated r/m was 9 times higher in S isolates (r/m = 4.4:1) than G isolates (r/m = 0.5:1). We did not detect a temporal signal when performing regression analysis (r) of tip-to-root distance versus isolation date, either in the entire collection (r = −0.2423) or for separate lineages (for G, r = −0.1314; for S, r = 0.1889) (Appendix). Hence, we could not determine when the 2 lineages diverged. The lack of temporal signal probably results from the limited number of isolates in each time point.

To further compare the 2 lineages, we constructed the pangenome of the 338 human *S. saprophyticus* genomes and identified 10,222 genes with 85% blastp clustering by using Roary. Among these, 8,351 genes,

present in <99% of the genomes, constituted the accessory genome. A gene accumulation plot of all the genes against the genomes sequenced showed that *S. saprophyticus* has an open pangenome (Appendix 2 Figure 2, panels A, B). The pan-GWAS analysis of the accessory genome indicated that G and S isolates have different genomic content (Bonferroni p<0.05, OR >1). A total of 128 genes were specific/enriched in the G lineage, including those encoding a type I restriction subunit (*group_383*), a defense mechanism against genetic transfer (*15*); metabolism of melibiose (*ebgA*, *melB*) (*16*) and inositol (*iolE*) (*17*), compounds that are excreted in urine; toxin–antitoxin systems (*group_4685*, *group_5665*), involved in stress response (*18*); and antimicrobial resistance (*qacA*) (*19*) (Table 1; Figure 5, panel A; Appendix 2 Table 1).

For S lineage, 237 genes were specific/enriched, some of which are involved in metabolism

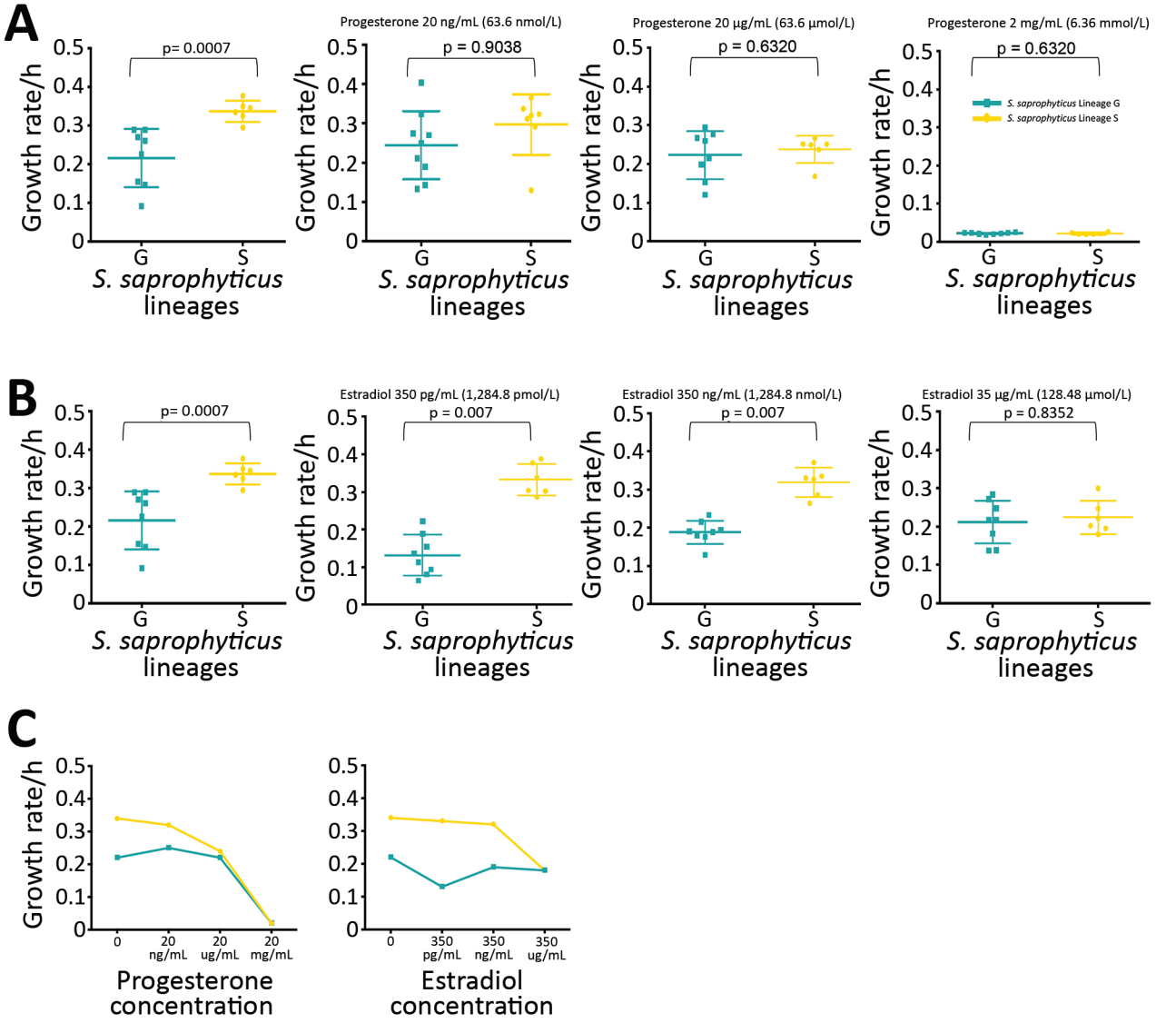

Figure 4. Growth rate of *Staphylococcus saprophyticus* clonal lineages in tryptic soy broth (TSB) and in different concentrations of female sex hormones. All assays were performed in triplicate and each experiment was repeated 3 times. A) Growth rate of *S. saprophyticus* strains in different concentrations of progesterone. First panel represents growth rate in TSB at 37°C; isolates belonging to lineage S grew significantly faster (p = 0.0007) than isolates in lineage G in TSB without hormones. However, no statistically significant difference in the growth rate of either lineage was noted in physiologic (2.0–200 ng/mL) and higher concentrations of progesterone. B) Growth rate of *S. saprophyticus* strains in TSB (first panel) and different concentrations of estradiol. Lineage S isolates grew faster in physiologic concentrations (350 pg/mL–350 ng/mL) and higher of estradiol, suggesting that this lineage is better adapted to the hormone-rich environment of the urine and the vagina than lineage G. Error bars indicate 95% CIs; horizontal lines indicate medians. C) Growth rate mean values of *S. saprophyticus* strains in progesterone and estradiol.

Table 1. List of genes exclusively associated with lineage G *Staphylococcus saprophyticus* strains in study of foodborne origin and local and global spread of *S. saprophyticus* causing human urinary tract infections*

Genes	Gene predicted function	Biologic function group	Frequency, %	Reference no.
group_383	Type I site-specific deoxyribonuclease restriction subunit	Endonuclease	96	(*15*)
icaR	Ica operon HTH-type negative transcription regulator	Transcription	95	NA
licT	Transcription antiterminator LicT	Transcription	80	NA
iolE	Inosose dehydratase	Inositol metabolism	86	(*17*)
group_4976	Phage infection protein	Phage-related protein	46	NA
group_869	Bacteriophage integrase	Phage-related protein	42	NA
tnpC_1	Transposase for transposon Tn*554*	Mobile genetic element	17	NA
group_744	Putative glucarate transporter	Transporter	29	NA
group_4685	Addiction module toxin Txe/YoeB family protein	Stress response (Type II toxin–antitoxin system)	20	(*18*)
group_5665	Addiction module antitoxin Axe family protein	Stress response (Type II toxin–antitoxin system)	19	(*18*)
yhjQ	Putative cysteine-rich protein YhjQ	Putative function	17	NA

*List of genes also include 53 hypothetical proteins. Bonferroni adjusted p≤0.032. NA, not applicable.

of ascorbate (*ulaA*) and thiamine (*tenI*) (*20*); induction of phosphate starvation (*psiE*), which was previously linked to switch on virulence in other uropathogens (*21*); platelet binding (*splE*, *sdrE*) associated with virulence (*22*); steroid metabolism (*group_7190*); and resistance to trimethoprim (*dfrG*) and biocides (*qacC*) (Table 2; Figure 5, panel A; Appendix 2 Table 1). Additional genes associated with S lineage that could explain its increased growth rate include those linked to lactose and cellobiose metabolism (*group_5572* gene) (*23*) and cell wall hydrolysis (*lytN*) (*24*), whereas the prevalence of transposases (*group_3547* and *group_1828*) (*25*) and phage genes (*recT* and *yueB*) (*27*) could justify its increased recombination rate.

Local and Global Spread of *S. saprophyticus* Clones Causing UTIs

We observed no time-based clustering of *S. saprophyticus* UTI isolates in the phylogeny, but we noted some geographic clustering. In particular, 89% (n = 78) of S isolates were found in Portugal and Spain (Figure 1). In addition, we identified clusters containing isolates from a single country. For instance, cluster G3 (1–8 SNPs) contained only isolates from Portugal and cluster G1 (0–63 SNPs) only isolates from Denmark (Figure 1).

We noted a high degree of isolate admixture in the maximum-likelihood tree of our global collection, suggesting that *S. saprophyticus* isolates of both lineages are disseminated geographically. G strains were distributed most widely, in 11 countries on 4 continents, whereas we found S isolates in only 6 countries. Despite the genetic diversity described, we still found isolates from different countries that differed by only a few SNPs. One pair in cluster G4 that had only 10 SNPs difference was a blood isolate from Barcelona, Spain (KS266), and a UTI isolate from Lisbon (KS135), collected in 2016 (Figure 1).

Although a relatedness cutoff is not defined yet for *S. saprophyticus*, the low number of SNPs observed between strains from the same and different countries is below the relatedness cutoff of 10–40 SNPs for most bacterial species (*28*). The apparent relatedness we noted implies that UTI isolates from different patients in the same country and in different countries are highly related and could belong to a cross-border chain of transmission. This finding challenges the assumption that *S. saprophyticus* causing UTIs were mainly endogenous (*29*).

Genetic Relatedness of *S. saprophyticus* from Slaughterhouses and UTIs

Pork is the most frequently consumed red meat in Europe (*30*) and is often contaminated with *S. saprophyticus* (*1*). We found that 35% of slaughterhouse samples (from meat, equipment, workers' hands, and a live pig) were contaminated with *S. saprophyticus*.

To understand whether *S. saprophyticus* causing UTIs could be related to *S. saprophyticus* in pork, we compared 104 isolates collected from a slaughterhouse against 128 isolates collected from human UTIs in Lisbon during 2016–2017. Among the 104 isolates from the slaughterhouse, 39 (37.5%) were collected from meat, 32 (30.8%) from equipment, 32 (30.8%) from workers' hands, and 1 (≈ 1%) from a live pig. SNP-based phylogenetic analysis with a tree-rooted at the midpoint showed that most (91%; 95/104) slaughterhouse isolates belonged to lineage G (Figure 2, panels A, B) and that a strain from slaughterhouse equipment was at the base of this lineage (bootstrap 100). In addition, the phylogenetic reconstruction including isolates from this study and other isolates

from production and companion animals (including 2 pigs, 2 bovine, and 1 canine) and food (*8*) showed that most (3/5) animal isolates clustered together at a basal clade of lineage G (bootstrap 100) (Appendix 2 Figure 2). Some clusters in the phylogenetic tree (e.g., G9) had slaughterhouse isolates at the base and UTI isolates at the tip. However, we also observed the opposite (e.g., G11), tree clusters with slaughterhouse isolates at the tip and UTI isolates at the base (Figure 2, panel A).Moreover, 41% of G strains included the antimicrobial resistance gene *tetK* ($p<0.0001$) (Figure 2, panel A), which is associated with resistance to tetracycline, an antimicrobial drug extensively used in animal production (*31*).

Phylogenetic reconstruction of all isolates from Lisbon based on SNPs provided additional examples of admixture of isolates recovered from different sampling sites in the slaughterhouse and from the slaughterhouse and humans. Isolates from meat were frequently intermixed with isolates from equipment and colonized workers as observed in cluster G6 wherein strains differed by only 1–65 SNPs (Figure 2, panel A; Figure 3). Likewise, cluster G9 included isolates from the slaughterhouse that were intermixed with human UTI isolates. Isolates collected from slaughterhouse equipment differed by only 19 SNPs from human UTI isolates. Likewise, human UTI isolates differed from meat isolates by 25 SNPs and from isolates of colonized workers by 26 SNPs. In addition, slaughterhouse and human UTI isolates had the same antimicrobial resistance profile, exhibiting resistance to fosfomycin, fusidic acid, and tetracycline (Appendix

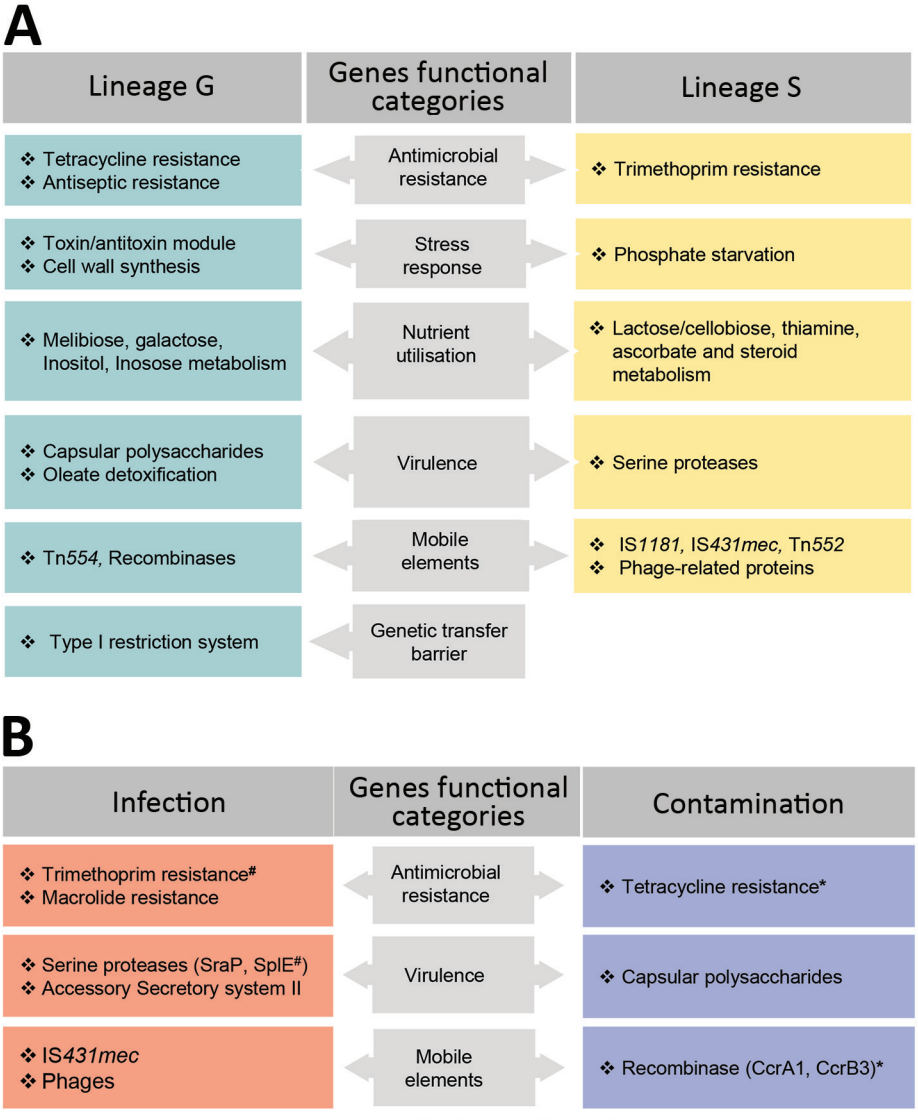

Figure 5. Genetic determinants that contribute to the distinction of clonal lineages and lifestyle of *Staphylococcus saprophyticus*. The graph displays determinants that contribute (A) and mediate (B) adaptation of *S. saprophyticus* to either infection or contamination. We used the genome-wide association study (GWAS) method to identify genetic factors by using 2 association comparisons: lineage G versus lineage S and human infection versus surface contamination. We used the pairwise comparison and included a core-SNP phylogenetic tree without recombination to remove the lineage effect in the analysis. Hits with Benjamini Hochberg corrected $p \leq 0.05$ and odds ratio >1 were considered statistically significant. We grouped the identified genes into biologic functions based on gene annotation predicted by Prokka (https://vicbioinformatics.com/software.prokka.shtml). Some genetic factors that were associated with infections and contamination also were associated with the lineages despite subjecting the GWAS to lineage correction.

Table 2. List of lineage S genes exclusively associated with *Staphylococcus saprophyticus* strains in study of foodborne origin and local and global spread of *S. saprophyticus* causing human urinary tract infections*

Genes	Gene predicted function	Biologic function group	Frequency, %	Reference no.
group_5572	Phosphotransferase system, lactose/ cellobiose-specific IIB subunit	Sugar metabolism	99	(*23*)
ulaA	PTS system ascorbate-specific IIC component	Sugar metabolism	99	(*20*)
group_5955	Sugar phosphate isomerase/epimerase	Sugar metabolism	26	(*23*)
lytN	C51 family D-Ala-D-Gly carboxypeptidase	Cell wall hydrolase	85	(*24*)
psiE	Protein PsiE	Phosphate starvation	22	(*21*)
group_1438	Arsenite methyltransferase	Arsenite resistance	25	NA
dfrG	Trimethoprim-resistance dihydrofolate reductase	Antimicrobial resistance	18	NA
group_7190	3-β hydroxysteroid dehydrogenase/isomerase	Steroid metabolism	17	(*26*)
group_273	Recombinase/resolvase	Mobile genetic element	69	(*25*)
group_2198	Putative ATPase/transposase	Mobile genetic element	26	(*25*)
group_275	Recombinase/resolvase	Mobile genetic element	21	(*25*)
group_355	Transposase for IS*431mec*	Mobile genetic element	17	(*25*)
group_7470	Putative replication-associated protein	Mobile genetic element	10	NA
group_3363	putative DoxX family membrane protein	Putative functions	85	NA
mviM	NADH-dependent dehydrogenase	Putative functions	26	NA
nmrA	Putative nmrA negative transcriptional regulator family protein	Transcription	17	NA
group_7195	Amidohydrolase	Hydrolase	17	NA
group_6430	Putative restriction enzyme	Restriction enzyme	17	NA

*List of genes also include 84 hypothetical proteins. Bonferroni p<0.031. NA, not applicable.

1 Table 1). We could not ascertain any epidemiologic link between the workers in the slaughterhouse and UTI patients, due to data protection limitations, but contact with meat production previously has been identified as a risk factor for UTI (*6*).

The only live-pig isolate was intermixed in cluster G8 with isolates from meat, slaughterhouse workers, and UTI patients (Figure 3), having 307–658 SNPs difference. The admixture of strains in the tree suggests the existence of frequent cross-transmission within the slaughterhouse and between the slaughterhouse and humans.

Insufficient disinfection procedures probably contributed to the high transmission rate of *S. saprophyticus* within the slaughterhouse, as demonstrated by the highly related strains (<11 SNPs) on dirty and clean equipment surfaces and similar strains (<16 SNPs) isolated 12 months apart. Carriage of the antimicrobial resistance gene, *qacA*, by all G strains could justify the observed unsuccessful cleaning procedures (Figure 2, panel A).

The accumulation of substitutions and genetic distance evidenced by the phylogenetic analysis suggest that isolates from slaughterhouses and food probably are the primary sources of *S. saprophyticus* G strains (Figure 3). Transmission probably occurs more frequently from the slaughterhouse and food to humans; however, we cannot ascertain directionality due to the lack of temporal signal.

Evidence Supporting the Human Origin of Lineage S

In contrast to isolates belonging to lineage G, which were mostly from UTIs and the slaughterhouse, S isolates were almost exclusively of human origin (97%; n = 66/68), either from UTIs (n = 59) or human colonization (n = 7) (Figure 2, panels A, B). When we reconstructed the phylogeny of all isolates in this and other studies (*8*) (Appendix 2 Figure 3), a human isolate was at the base of the S lineage. The only 2 S isolates seen in animals were from nonhuman primates. Furthermore, a resistance determinant for trimethoprim (*dfrG*), which routinely is used to treat human UTIs, was associated with this lineage (18%; p<0.05) (Figure 2, panel A; Table 2).

To determine whether S isolates could have originated in humans, we grew isolates from both lineages in the absence and presence of human physiologic concentrations (15–350 pg/mL) of estradiol (*32*), a female hormone commonly found in urine and the vagina, and in different pH values mimicking the stomach (pH 2.5), vagina (pH ≤4.5) (*33*), skin (pH 5.5), and urine (pH 4.5–8.0) (*34*). The growth rate of S isolates did not change significantly at the highest physiologic concentration of estradiol specific to humans (0.34 h^{-1} vs. 0.33 h^{-1}), but the growth rate for G strains decreased by 59% at this concentration (0.22 h^{-1} vs. 0.13 h^{-1}; p = 0.0007) (Figure 4, panels A–C; Appendix 2). All isolates grew at all pH levels assayed, except for pH 2.5. At pH 4.5 and 5.5, isolates of both lineages had similar growth rates, but S isolates had a higher growth rate than G isolates at pH 8, although this difference was not statistically significant (p = 0.133). These results suggest that lineage S isolates are more adapted than lineage G strains to high estradiol concentrations found in women, but not found in other female animal hosts, such as pigs, bovine, or canines (*35*). GWAS also identified a gene involved in

steroid metabolism, 3-β hydroxysteroid dehydrogenase (HSD), associated with lineage S (Table 2; Figure 5, panels A, B). Steroids such as estradiol are primary signaling molecules for host–microbe interactions (*26*) and involved in the interconversion of active and inactive steroid hormones (*26*). Presence of HSD could be an adaptive evolution to colonization of the bladder, a hormone-rich environment. Evidence supports a human (primate) origin for lineage S, but studies sampling a wider range of ecologic sites and geographic regions are needed.

UTIs and *S. saprophyticus* Dissemination among Humans in the Community

To explore dissemination of *S. saprophyticus* causing UTIs in the community through human-to-human contact, we analyzed genomic data of the 128 UTI isolates from outpatients of 3 hospitals in the Lisbon area. Transmission of *S. saprophyticus* from lineage G and S between persons in the community was apparent, as demonstrated by the high relatedness of strains from UTI patients at different hospitals. In the G cluster, G10 isolates had 9–24 SNPs difference, and in the S cluster, S2, differed by 6–64 SNPs (Figure 2, panel A). However, due to data protection regulations, we could not ascertain whether the patients were epidemiologically linked. Results suggest that patients might have acquired these strains from the same reservoir or that direct and indirect cross-transmission could have occurred in the community.

Disease Signatures among *S. saprophyticus* Populations

Several virulence factors, including urease, have been described in *S. saprophyticus* (*36*), but the basis of pathogenicity in this species is mainly unknown. We used a pan-GWAS approach to compare the genetic content of 128 isolates from human infections to 104 isolates recovered from a slaughterhouse, all collected in Lisbon during 2016–2017. We identified 6 genes that appear to be associated with an increased pathogenic potential in *S. saprophyticus* (Figure 5, panel A; Appendix 2 Tables 2–5). These genes included those encoding an SplE-like protein and a gene cluster encoding a complete accessory secretory system associated with a serine-rich adhesion, similar to SraP. Previous studies have described highly homologous secretory system (>97% nucleotide identity) associated to serine-rich proteins that bind platelets, including SraP in *S. aureus* (*37*) and UafB in *S. saprophyticus* (*38*).

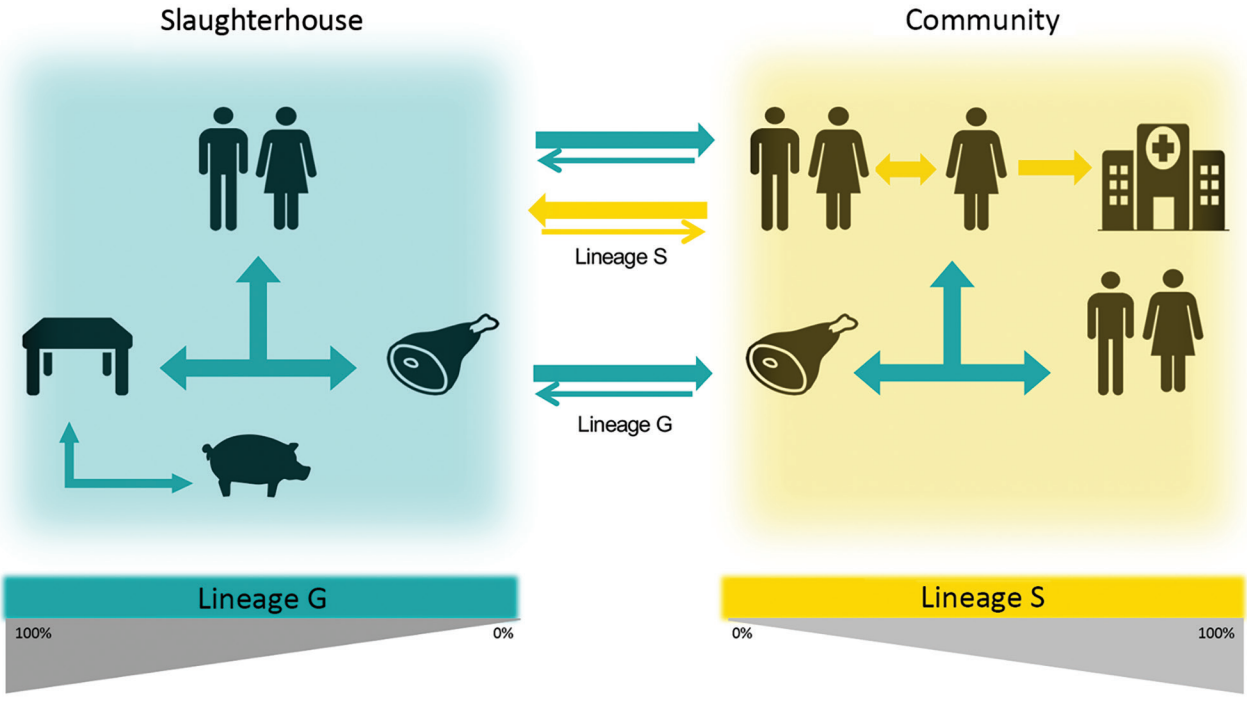

Figure 6. A proposed model for the dissemination and transmission of *Staphylococcus saprophyticus* in the community. The arrows represent the dissemination and transmission of *S. saprophyticus* isolates that belonged to lineage G (green) and lineage S (yellow). Lineage G *S. saprophyticus* strains are of animal origin and enter the slaughterhouse through production animals, such as pigs, persist on the equipment, and contaminate the meat in processing chain. Lineage G strains could enter the community through contaminated meat and workers colonized in the slaughterhouse. Lineage S strains most likely are of humans and primate origin and probably are disseminated by person-to-person contact within the community.

We also found other genes associated with infection that encoded phage proteins. An analysis on 128 UTI isolates using PHASTER (*39*) identified 5 phages in 48 (38%) strains. The phages were 38–125 Kb and had <50% identity with any known phage. The genomic vicinity of the identified phages varied in the chromosome, suggesting that lysogenic conversion was not the mechanism involved in pathogenicity of these strains; instead, hypothetical phage genes could be crucial for pathogenicity. In addition, genes encoding resistance to the antimicrobial drugs trimethoprim (*dfrG*), lincosamide (*lnuA*), streptogramin B (*erm44v*), or to macrolides (*mphC-msrA*) also were associated with strains from human infections (Figure 2; Figure 5, panel B; Appendix 2 Tables 2–5).

Another factor highly associated with human infections was the occurrence of recombination, which was 6 times higher in isolates from UTIs (r/m 1.7:1) than from isolates associated with colonization or contamination (r/m 0.3:1). This finding suggests recombination might be a strategy of *S. saprophyticus* to evade the host immune system, as described elsewhere (*40*).

Discussion

We identified 2 *S. saprophyticus* lineages, G and S, associated with human UTIs that appeared to have different evolutionary histories. Our data support a foodborne origin for lineage G and its transmission through food products to humans. We also found evidence of a human origin for lineage S and additional proof for the occurrence of direct or indirect human-to-human dissemination in the community, which could explain not only the local dissemination of both lineages but also the wide geographic dissemination, as described for *S. aureus* (*41*) and *E. coli* (*42*).

Our conclusions were limited by the characteristics of the sample collection analyzed. In particular, the lack of temporal signal did not enable inference of the direction of transmission between the sampling sites. We could establish obvious genomic relatedness between the meat production chain and human UTIs and UTIs from different persons in the community. However, lack of samples from other animal hosts, environments, or different ecologic niches in humans, did not enable us to establish pig meat and humans as the unique sources of the 2 lineages nor identify the preferred ecologic niche of *S. saprophyticus* in humans.

Our observed *S. saprophyticus* colonization rate among pigs was extremely low (1%) compared with previous studies (*43*), which could be explained by possible cross-inhibitory bacterial interactions (*44*); however, contamination within the slaughterhouse environment sometimes reached 35%. Amplification of *S. saprophyticus* in the slaughterhouse environment was probably potentiated by resistance to biocides. We found that slaughterhouse workers' washed hands were colonized with strains that were highly related to slaughterhouse environmental isolates and to strains causing UTIs, suggesting exposure of workers to the slaughterhouse environment as a risk factor for human colonization (Figure 6).

The transmission chain of S lineage isolates appears to be different and to have no link to meat production. S lineage UTIs might originate from human gut or vaginal colonization; both have been reported as possible human niches (*2*,*4*). Evidence for the human origin of S lineage included the almost exclusive (97%) identification in humans, where S lineage was better adapted to the physiologic high concentration of human female sex hormones; grew at vagina, skin, and urine pH values; and harbored 2 serine-proteases that presumably can bind to human platelets, as described for SraP (*37*). The distinct genetic content and phenotypic features of lineages G and S further reflected the diverse selective pressures of the human and animal, slaughterhouse, and food environments and suggest different evolutionary strategies toward pathogenicity. In particular, we found that tetracycline and antimicrobial resistance genes associated with colonization-contamination also were associated with isolates of the G lineage. Furthermore, genes encoding sugar metabolism, serine proteases, and a trimethoprim resistance associated with infection were also associated with isolates of the S lineage, implying distinctive specialization of the 2 lineages.

Our results also indicate a key role of setting-associated antimicrobial drug usage, especially for trimethoprim, macrolides, and tetracycline, in resistance development and pathogenicity. Subinhibitory concentrations of these drugs have been shown to promote virulence in bacteria through the induction of biofilm production (*45*), quorum-sensing (*45*), or phages (*46*) and might also increase *S. saprophyticus* pathogenicity.

We found a high r/m rate in isolates of the S lineage and in strains from UTIs, comparable to naturally transformable bacterial species like *Klebsiella pneumoniae* and *Streptococcus pyogenes* (*47*). A similar phenomenon was observed for *S. epidermidis* (*48*); variation in cell surface proteins was shown to contribute to evasion of human immunity (*48*), and a similar strategy might be advantageous for *S. saprophyticus* in infection. The recombination might have resulted from defects in repair of double stranded DNA breaks from

oxidative stress induced by leukocytes during infection, as previously described (*48*). However, the mechanism linking infection and recombination in *S. saprophyticus* remains elusive.

Last, we identified factors associated with infection that could represent new *S. saprophyticus* virulence factors, including 2 serine-proteases, *sraP*-like and *splE*-like, and phages SraP and SplE, which previously were connected to pathogenicity in *S. aureus* (*22*,*37*). In addition, phages have been described to transport pathogenicity islands in staphylococci (*49*). Our study constitutes a deep-structured analysis of *S. saprophyticus* population structure and genomic epidemiology, providing groundwork for future studies on the pathogenicity and population genetics of this bacterium.

O.U.L. was supported by PhD grants from the Fundação para a Ciência e Tecnologia (FCT) (grant no. PD/BD/113992/2015). This work was partially supported by FCT (project no. PTDC/CVT-CVT/29510/2017), Microbiologia Molecular, Estrutural e Celular (project nos. LISBOA-01-0145-FEDER-007660 and UID/Multi/04378/2019) and by the COMPETE2020 Programa Operacional Competitividade e Internacionalização; ONEIDA (project no. LISBOA-01-0145-FEDER-016417), and co-funded by Fundos Europeus Estruturais e de Investimento from Programa Operacional Regional Lisboa2020 and by national funds through FCT.

O.U.L. and O.B. cultured the isolates. O.U.L. performed the phenotypic experiments and bioinformatics analysis. O.U.L., H.W., P.W., M.D.B. performed the sequencing of the isolates. O.U.L. and M.M. carried out the data analysis and interpretation and wrote the manuscript. M.J.F., M.L.G., P.P., E.G., C.T., J.E., M.U., H.M.L., H.W., M.D.B. provided the isolates. M.J.F., M.L.G., P.P., E.G., C.T., J.E., M.U., H.M.L., H.W., P.W., M.D.B. were involved in manuscript revision. All authors read and approved the final manuscript.

About the Author

Dr. Lawal is a postdoctoral researcher at the Instituto de Tecnologia Quimica e Biologica, Universidade Nova de Lisboa (ITQB-NOVA), Oeiras, Portugal. His primary research interests include antimicrobial resistance, bacterial evolution and transmission dynamics of *Staphylococcus saprophyticus*.

References

1. Becker K, Heilmann C, Peters G. Coagulase-negative staphylococci. Clin Microbiol Rev. 2014;27:870–926. https://doi.org/10.1128/CMR.00109-13
2. Latham RH, Running K, Stamm WE. Urinary tract infections in young adult women caused by *Staphylococcus saprophyticus*. JAMA. 1983;250:3063–6. https://doi.org/10.1001/jama.1983.03340220031028
3. Garduño E, Márquez I, Beteta A, Said I, Blanco J, Pineda T. *Staphylococcus saprophyticus* causing native valve endocarditis. Scand J Infect Dis. 2005;37:690–1. https://doi.org/10.1080/00365540510027200
4. Rupp ME, Soper DE, Archer GL. Colonization of the female genital tract with *Staphylococcus saprophyticus*. J Clin Microbiol. 1992;30:2975–9. https://doi.org/10.1128/JCM.30.11.2975-2979.1992
5. de Sousa VS, da-Silva APS, Sorenson L, Paschoal RP, Rabello RF, Campana EH, et al. *Staphylococcus saprophyticus* recovered from humans, food, and recreational waters in Rio de Janeiro, Brazil. Int J Microbiol. 2017;2017:4287547. https://doi.org/10.1155/2017/4287547
6. Hedman P, Ringertz O, Eriksson B, Kvarnfors P, Andersson M, Bengtsson L, et al. *Staphylococcus saprophyticus* found to be a common contaminant of food. J Infect. 1990;21:11–9. https://doi.org/10.1016/0163-4453(90)90554-L
7. Lee B, Jeong D-W, Lee J-H. Genetic diversity and antibiotic resistance of *Staphylococcus saprophyticus* isolates from fermented foods and clinical samples. J Korean Soc Appl Biol Chem. 2015;58:659–68. https://doi.org/10.1007/s13765-015-0091-1
8. Mortimer TD, Annis DS, O'Neill MB, Bohr LL, Smith TM, Poinar HN, et al. Adaptation in a fibronectin binding autolysin of *Staphylococcus saprophyticus*. MSphere. 2017;2:e00511–17. https://doi.org/10.1128/mSphere.00511-17
9. Kuroda M, Yamashita A, Hirakawa H, Kumano M, Morikawa K, Higashide M, et al. Whole genome sequence of *Staphylococcus saprophyticus* reveals the pathogenesis of uncomplicated urinary tract infection. Proc Natl Acad Sci U S A. 2005;102:13272–7. PubMed https://doi.org/10.1073/pnas.0502950102
10. Hansen KH, Andreasen MR, Pedersen MS, Westh H, Jelsbak L, Schønning K. Resistance to piperacillin/tazobactam in *Escherichia coli* resulting from extensive IS*26*-associated gene amplification of *blaTEM-1*. J Antimicrob Chemother. 2019;74:3179–83. https://doi.org/10.1093/jac/dkz349
11. Kaas RS, Leekitcharoenphon P, Aarestrup FM, Lund O. Solving the problem of comparing whole bacterial genomes across different sequencing platforms. PLoS One. 2014;9:e104984. https://doi.org/10.1371/journal.pone.0104984
12. Croucher NJ, Page AJ, Connor TR, Delaney AJ, Keane JA, Bentley SD, et al. Rapid phylogenetic analysis of large samples of recombinant bacterial whole genome sequences using Gubbins. Nucleic Acids Res. 2015;43:e15. https://doi.org/10.1093/nar/gku1196
13. Brynildsrud O, Bohlin J, Scheffer L, Eldholm V. Erratum to: Rapid scoring of genes in microbial pan-genome-wide association studies with Scoary. Genome Biol. 2016;17:1–9. https://doi.org/10.1186/s13059-016-1108-8
14. Chen L, Zheng D, Liu B, Yang J, Jin Q. VFDB 2016: hierarchical and refined dataset for big data analysis—10 years on. Nucleic Acids Res. 2016;44(D1):D694–7. https://doi.org/10.1093/nar/gkv1239
15. Monk IR, Foster TJ. Genetic manipulation of Staphylococci-breaking through the barrier. Front Cell Infect Microbiol. 2012;2:49. https://doi.org/10.3389/fcimb.2012.00049
16. Tomita K, Nagura T, Okuhara Y, Nakajima-Adachi H, Shigematsu N, Aritsuka T, et al. Dietary melibiose regulates the cell response and enhances the induction of oral

tolerance. Biosci Biotechnol Biochem. 2007;71:2774–80. https://doi.org/10.1271/bbb.70372
17. Dinicola S, Minini M, Unfer V, Verna R, Cucina A, Bizzarri M. Nutritional and acquired deficiencies in inositol bioavailability. Correlations with metabolic disorders. Int J Mol Sci. 2017;18:E2187. https://doi.org/10.3390/ijms18102187
18. Gómez FA, Cárdenas C, Henríquez V, Marshall SH. Characterization of a functional toxin-antitoxin module in the genome of the fish pathogen *Piscirickettsia salmonis*. FEMS Microbiol Lett. 2011;317:83–92. https://doi.org/10.1111/j.1574-6968.2011.02218.x
19. Conceição T, Coelho C, de Lencastre H, Aires-de-Sousa M. High prevalence of biocide resistance determinants in *Staphylococcus aureus* isolates from three African countries. Antimicrob Agents Chemother. 2015;60:678–81. https://doi.org/10.1128/AAC.02140-15
20. Costliow ZA, Degnan PH. Thiamine acquisition strategies impact metabolism and competition in the gut microbe *Bacteroides thetaiotaomicron*. mSystems. 2017;2:1–17. https://doi.org/10.1128/mSystems.00116-17
21. Chekabab SM, Harel J, Dozois CM. Interplay between genetic regulation of phosphate homeostasis and bacterial virulence. Virulence. 2014;5:786–93. https://doi.org/10.4161/viru.29307
22. Sharp JA, Echague CG, Hair PS, Ward MD, Nyalwidhe JO, Geoghegan JA, et al. Staphylococcus aureus surface protein SdrE binds complement regulator factor H as an immune evasion tactic. PLoS One. 2012;7:e38407. https://doi.org/10.1371/journal.pone.0038407
23. Ghali I, Sofyan A, Ohmori H, Shinkai T, Mitsumori M. Diauxic growth of *Fibrobacter succinogenes* S85 on cellobiose and lactose. FEMS Microbiol Lett. 2017;364:1–9. https://doi.org/10.1093/femsle/fnx150
24. Frankel MB, Hendrickx APA, Missiakas DM, Schneewind O. LytN, a murein hydrolase in the cross-wall compartment of *Staphylococcus aureus*, is involved in proper bacterial growth and envelope assembly. J Biol Chem. 2011;286:32593–605. https://doi.org/10.1074/jbc.M111.258863
25. Hallet B, Sherratt DJ. Transposition and site-specific recombination: adapting DNA cut-and-paste mechanisms to a variety of genetic rearrangements. FEMS Microbiol Rev. 1997;21:157–78. https://doi.org/10.1111/j.1574-6976.1997.tb00349.x
26. García-Gómez E, González-Pedrajo B, Camacho-Arroyo I. Role of sex steroid hormones in bacterial-host interactions. BioMed Res Int. 2013;2013:928290. https://doi.org/10.1155/2013/928290
27. Datta S, Costantino N, Zhou X, Court DL. Identification and analysis of recombineering functions from Gram-negative and Gram-positive bacteria and their phages. Proc Natl Acad Sci U S A. 2008;105:1626–31. https://doi.org/10.1073/pnas.0709089105
28. Schürch AC, Arredondo-Alonso S, Willems RJL, Goering RV. Whole genome sequencing options for bacterial strain typing and epidemiologic analysis based on single nucleotide polymorphism versus gene-by-gene-based approaches. Clin Microbiol Infect. 2018;24:350–4. https://doi.org/10.1016/j.cmi.2017.12.016
29. Ronald A. The etiology of urinary tract infection: traditional and emerging pathogens. Dis Mon. 2003;49:71–82. https://doi.org/10.1067/mda.2003.8
30. González-García S, Belo S, Dias AC, Rodrigues JV, Da Costa RR, Ferreira A, et al. Life cycle assessment of pigmeat production: Portuguese case study and proposal of improvement options. J Clean Prod. 2015;100:126–39. https://doi.org/10.1016/j.jclepro.2015.03.048
31. Chopra I, Roberts M. Tetracycline antibiotics: mode of action, applications, molecular biology, and epidemiology of bacterial resistance. Microbiol Mol Biol Rev. 2001;65:232–60. https://doi.org/10.1128/MMBR.65.2.232-260.2001
32. Walker SW. Laboratory reference ranges. In: Endocrine self-assessment program. Washington, D.C.: Endocrine Society; 2015. p. 1–5 [cited 2019 Apr 29]. https://education.endocrine.org/system/files/ESAP%202015%20Laboratory%20Reference%20Ranges.pdf
33. Linhares IM, Minis E, Robial R, Witkin SS. The human vaginal microbiome. In: Faintuch J, Faintuch S, editors. Microbiome and metabolome in diagnosis, therapy, and other strategic applications. London: Elsevier, Inc.; 2019. p. 109–14. https://doi.org/10.1016/B978-0-12-815249-2.00011-7
34. Clarkson MR, Magee CN, Brenner BM. Chapter 2: Laboratory assessment of kidney disease. In: Clarkson MR, Magee CN, Brenner BM eds. Pocket companion to Brenner and Rector's the Kidney 8th edition. London: Elsevier; 2011. p. 21–41 [cited 2019 Apr 29]. https://www.sciencedirect.com/science/article/pii/B9781416066408000026
35. Frank LA, Mullins R, Rohrbach BW. Variability of estradiol concentration in normal dogs. Vet Dermatol. 2010;21:490–3. https://doi.org/10.1111/j.1365-3164.2010.00896.x
36. Flores-Mireles AL, Walker JN, Caparon M, Hultgren SJ. Urinary tract infections: epidemiology, mechanisms of infection and treatment options. Nat Rev Microbiol. 2015;13:269–84. https://doi.org/10.1038/nrmicro3432
37. Siboo IR, Chaffin DO, Rubens CE, Sullam PM. Characterization of the accessory *Sec* system of *Staphylococcus aureus*. J Bacteriol. 2008;190:6188–96. https://doi.org/10.1128/JB.00300-08
38. King NP, Beatson SA, Totsika M, Ulett GC, Alm RA, Manning PA, et al. UafB is a serine-rich repeat adhesin of *Staphylococcus saprophyticus* that mediates binding to fibronectin, fibrinogen and human uroepithelial cells. Microbiology (Reading). 2011;157:1161–75. https://doi.org/10.1099/mic.0.047639-0
39. Arndt D, Grant JR, Marcu A, Sajed T, Pon A, Liang Y, et al. PHASTER: a better, faster version of the PHAST phage search tool. Nucleic Acids Res. 2016;44:W16–21. https://doi.org/10.1093/nar/gkw387
40. Yahara K, Didelot X, Jolley KA, Kobayashi I, Maiden MCJ, Sheppard SK, et al. The landscape of realized homologous recombination in pathogenic bacteria. Mol Biol Evol. 2016;33:456–71. https://doi.org/10.1093/molbev/msv237
41. Tristan A, Bes M, Meugnier H, Lina G, Bozdogan B, Courvalin P, et al. Global distribution of Panton-Valentine leukocidin—positive methicillin-resistant *Staphylococcus aureus*, 2006. Emerg Infect Dis. 2007;13:594–600. https://doi.org/10.3201/eid1304.061316
42. Vincent C, Boerlin P, Daignault D, Dozois CM, Dutil L, Galanakis C, et al. Food reservoir for *Escherichia coli* causing urinary tract infections. Emerg Infect Dis. 2010;16:88–95. https://doi.org/10.3201/eid1601.091118
43. Hedman P, Ringertz O, Lindström M, Olsson K. The origin of *Staphylococcus saprophyticus* from cattle and pigs. Scand J Infect Dis. 1993;25:57–60. https://doi.org/10.1080/00365549309169670
44. Verstappen KM, Willems E, Fluit AC, Duim B, Martens M, Wagenaar JA. *Staphylococcus aureus* nasal colonization differs among pig lineages and is associated with the presence of other staphylococcal species. Front Vet Sci. 2017;4:97. https://doi.org/10.3389/fvets.2017.00097
45. Imperi F, Leoni L, Visca P. Antivirulence activity of azithromycin in *Pseudomonas aeruginosa*. Front Microbiol. 2014;5:178. https://doi.org/10.3389/fmicb.2014.00178

46. Goerke C, Köller J, Wolz C. Ciprofloxacin and trimethoprim cause phage induction and virulence modulation in *Staphylococcus aureus*. Antimicrob Agents Chemother. 2006; 50:171–7. https://doi.org/10.1128/AAC.50.1.171-177.2006
47. Davies MR, McIntyre L, Mutreja A, Lacey JA, Lees JA, Towers RJ, et al. Atlas of group A streptococcal vaccine candidates compiled using large-scale comparative genomics. Nat Genet. 2019;51:1035–43. https://doi.org/10.1038/s41588-019-0417-8
48. Méric G, Mageiros L, Pensar J, Laabei M, Yahara K, Pascoe B, et al. Disease-associated genotypes of the commensal skin bacterium *Staphylococcus epidermidis*. Nat Commun. 2018;9:5034. https://doi.org/10.1038/s41467-018-07368-7
49. Dearborn AD, Dokland T. Mobilization of pathogenicity islands by *Staphylococcus aureus* strain Newman bacteriophages. Bacteriophage. 2012;2:70–8. https://doi.org/10.4161/bact.20632

Address for correspondence: Maria Miragaia, Laboratory of Bacterial Evolution and Molecular Epidemiology, Instituto de Tecnologia Química e Biológica, Universidade Nova de Lisboa (ITQB-NOVA), Avenida da República, 2780-157, Oeiras, Portugal; email: miragaia@itqb.unl.pt

Article DOI: https://doi.org/10.3201/eid2703.200852

Foodborne Origin and Local and Global Spread of *Staphylococcus saprophyticus* Causing Human Urinary Tract Infections

Appendix 2

Supplementary Methods

Bacterial Isolates

In addition to the global and local *Staphylococcus saprophyticus* collections stated in the manuscript, we included *S. saprophyticus* isolates from food production animals (1 pig and 3 bovine), 1 companion canine, 12 food isolates, and 1 isolate recovered from a river, which was described in previous studies (*1*). We also included 18 *S. saprophyticus* isolates recovered from food products and 2 isolates from nonhuman primates from our collection. These isolates, together with the global and local collection (n = 480) was analyzed to infer the origin of the *S. saprophyticus* lineages.

Isolation and Species Identification of Slaughterhouse Isolates

We enriched samples in peptone water and grew isolates on CHROMagar Staph aureus (CHROMagar Microbiology, https://www.chromagar.com) supplemented with 10% NaCl and 4 µg/mL novobiocin. We extracted genomic DNA by using methods previously described (*2*). We performed species identification by amplifying and sequencing the *tuf* gene (*3*).

Growth Rate in Different pH and Hormones

For representative isolates from the collection, we performed growth curves at different concentrations of female sex hormones, including progesterone at 20 ng/mL, 20 µg/mL, and 20 mg/mL, and estradiol at 350 pg/mL, 350 ng/mL, and 350 µg/mL; and at pH levels of 2.5, 4.5, 5.5, and 8.0. We performed growth assays by using an Infinite 200 PRO series microtiter reader (Tecan Group Ltd, https://www.tecan.com) in 96-well microtiter plates. For each strain, overnight culture was inoculated onto 5 mL Bacto tryptic soy broth (TSB; Becton Dickinson,

https://www.bd.com). The OD_{600nm} of the liquid culture was adjusted to an initial OD of 0.5 MacFarland with buffers for specific pHs and TSB containing varying concentrations of hormones and grown with aeration (180 rpm) at 37°C for 18 h. Assays were performed in triplicate and each experiment was repeated 3 times.

Estimation of Evolutionary Rates

To estimate the evolutionary rates in *S. saprophyticus* population, as a first approach, we explored the degree and pattern of temporal signal and determined whether sufficient temporal signals were available in the *S. saprophyticus* phylogeny. We performed a regression of the divergence of each tip from the root against the date of sampling, a root-to-tip plot, of the global collection and separately for the lineages using TempEst v1.5.3 (*4*). We used the phylogenetic tree without recombination and the date of isolation of the isolates as inputs.

Average Nucleotide Identity Analysis

We calculated average nucleotide identity (ANI) for representative strains of *S. saprophyticus* 40 G lineages and 20 S lineages by using a standalone Python program, pyani version 0.2.9 (https://github.com/widdowquinn/pyani) and the ANIb option, which compares genomes using BLAST program (https://blast.ncbi.nlm.nih.gov). The closed genome of KS40 was used as a reference for lineage G and closed genome of KS160 was used for lineage S.

Intrasample Diversity

We assessed the genetic diversity between isolates recovered from the same sample in the meat processing chain. We determined whether intrasample diversity existed by comparing the SNP differences between these isolates.

Data Availability

All raw sequence data are available in the SRA (https://www.ncbi.nlm.nih.gov/sra) under the study accession no. PRJNA604222. We also provide individual accession numbers for raw sequence data (Appendix 1 Table 1) and the SNP matrices and list of genes in the pangenomes (Appendix 1 Tables 2–6).

Results

Pangenome Analysis of *S. saprophyticus* Revealed an Open Pangenome

We annotated the 338 *S. saprophyticus* genomes by using Prokka (*5*) and constructed the pangenome by using Roary (*6*) with 85% blastp identity. A total of 10,222 genes were found, 48% (n = 4,925) of which were genes with unknown functions. The genes constituting the core of all isolates consisted of 1,871 genes. Also, we noted 118 soft core genes in 95%–99% of the isolates, 856 shell genes in 15%–94%, and we found 7,307 genes that constituted cloud genes in <15% of *S. saprophyticus* population. On average, 75% of *S. saprophyticus* genome is constituted by core genes and 25% of accessory genes. The plot of the total number of genes against the number of genomes indicate an open pangenome in which each genome sequence added several new genes. This finding implies that newly sequenced genomes will identify new genes and the pangenome size of this species will continue to increase (Appendix 2 Figure 2).

GWAS Revealed Genetic Factors Associated with *S. saprophyticus* Isolates from Different Genetic Lineages and Clinical Origins

We explored the pangenome gene presence to understand the difference in the genetic content of isolates from each of the genetic lineages defined by core SNPs. We used Scoary pipeline (*7*) and Bonferroni $p<0.05$ to identify genes that were exclusive or enriched in the *S. saprophyticus* genetic lineages. We categorized the hits into biologic function groups based on the annotations predicted by Prokka. For genes associated with different clinical origins (infection and colonization/contamination), we used Benjamini Hochberg and pairwise $p<0.05$ (Appendix 2 Tables 1–5).

References

1. Mortimer TD, Annis DS, O'Neill MB, Bohr LL, Smith TM, Poinar HN, et al. Adaptation in a fibronectin binding autolysin of *Staphylococcus saprophyticus.* MSphere. 2017;2:e00511–17. PubMed https://doi.org/10.1128/mSphere.00511-17

2. Couto I, Pereira S, Miragaia M, Sanches IS, de Lencastre H. Identification of clinical staphylococcal isolates from humans by internal transcribed spacer PCR. J Clin Microbiol. 2001;39:3099–103. PubMed https://doi.org/10.1128/JCM.39.9.3099-3103.2001

3. Martineau F, Picard FJ, Ménard C, Roy PH, Ouellette M, Bergeron MG. Development of a rapid PCR assay specific for *Staphylococcus saprophyticus* and application to direct detection from urine

samples. J Clin Microbial. 2000;38:3280–4. PubMed https://doi.org/10.1128/JCM.38.9.3280-3284.2000

4. Rambaut A, Lam TT, Max Carvalho L, Pybus OG. Exploring the temporal structure of heterochronous sequences using TempEst (formerly Path-O-Gen). Virus Evol. 2016;2:vew007. PubMed https://doi.org/10.1093/ve/vew007

5. Seemann T. Prokka: rapid prokaryotic genome annotation. Bioinformatics. 2014;30:2068–9. PubMed https://doi.org/10.1093/bioinformatics/btu153

6. Page AJ, Cummins CA, Hunt M, Wong VK, Reuter S, Holden MTG, et al. Roary: rapid large-scale prokaryote pan genome analysis. Bioinformatics. 2015;31:3691–3. PubMed https://doi.org/10.1093/bioinformatics/btv421

7. Brynildsrud O, Bohlin J, Scheffer L, Eldholm V. Erratum to: Rapid scoring of genes in microbial pan-genome-wide association studies with Scoary. Genome Biol. 2016;17:1–9. PubMed https://doi.org/10.1186/s13059-016-1108-8

8. Tomita K, Nagura T, Okuhara Y, Nakajima-Adachi H, Shigematsu N, Aritsuka T, et al. Dietary melibiose regulates the cell response and enhances the induction of oral tolerance. Biosci Biotechnol Biochem. 2007;71:2774–80. PubMed https://doi.org/10.1271/bbb.70372

9. Costliow ZA, Degnan PH. Thiamine acquisition strategies impact metabolism and competition in the gut microbe *Bacteroides thetaiotaomicron.* [Internet]. mSystems. 2017;2:1–17 http://msystems.asm.org/lookup/doi/10.1128/mSystems.00116-17. PubMed https://doi.org/10.1128/mSystems.00116-17

10. Sharp JA, Echague CG, Hair PS, Ward MD, Nyalwidhe JO, Geoghegan JA, et al. Staphylococcus aureus surface protein SdrE binds complement regulator factor H as an immune evasion tactic. PLoS One. 2012;7:e38407. PubMed https://doi.org/10.1371/journal.pone.0038407

11. Hallet B, Sherratt DJ. Transposition and site-specific recombination: adapting DNA cut-and-paste mechanisms to a variety of genetic rearrangements. FEMS Microbiol Rev. 1997;21:157–78. PubMed https://doi.org/10.1111/j.1574-6976.1997.tb00349.x

12. Datta S, Costantino N, Zhou X, Court DL. Identification and analysis of recombineering functions from Gram-negative and Gram-positive bacteria and their phages. Proc Natl Acad Sci U S A. 2008;105:1626–31. PubMed https://doi.org/10.1073/pnas.0709089105

13. Imperi F, Leoni L, Visca P. Antivirulence activity of azithromycin in *Pseudomonas aeruginosa.* Front Microbiol. 2014;5:178. PubMed https://doi.org/10.3389/fmicb.2014.00178

14. Goerke C, Köller J, Wolz C. Ciprofloxacin and trimethoprim cause phage induction and virulence modulation in *Staphylococcus aureus*. Antimicrob Agents Chemother. 2006;50:171–7. PubMed https://doi.org/10.1128/AAC.50.1.171-177.2006

15. Siboo IR, Chaffin DO, Rubens CE, Sullam PM. Characterization of the accessory *Sec* system of *Staphylococcus aureus*. J Bacteriol. 2008;190:6188–96. PubMed https://doi.org/10.1128/JB.00300-08

16. King NP, Beatson SA, Totsika M, Ulett GC, Alm RA, Manning PA, et al. UafB is a serine-rich repeat adhesin of *Staphylococcus saprophyticus* that mediates binding to fibronectin, fibrinogen and human uroepithelial cells. Microbiology (Reading). 2011;157:1161–75. PubMed https://doi.org/10.1099/mic.0.047639-0

17. Monk IR, Foster TJ. Genetic manipulation of Staphylococci-breaking through the barrier. Front Cell Infect Microbiol. 2012;2:49. PubMed https://doi.org/10.3389/fcimb.2012.00049

18. Chopra I, Roberts M. Tetracycline antibiotics: mode of action, applications, molecular biology, and epidemiology of bacterial resistance. Microbiol Mol Biol Rev. 2001;65:232–60. PubMed https://doi.org/10.1128/MMBR.65.2.232-260.2001

Appendix 2 Table 1. List of differentially enriched genes in *Staphylococcus saprophyticus* lineages in a study of isolates from human urinary tract infections and meat processing plants*

Gene	Gene predicted function	Biologic function group	Lineage G, %	Lineage S, %	Reference no.
melB	Melibiose carrier protein	Sugar transport and metabolism	98	26	(*8*)
ebgA	Evolved β-galactosidase subunit α	Sugar transport and metabolism	98	26	(*8*)
csxA	Exo-β-D-glucosaminidase	Sugar transport and metabolism	62	1	(*8*)
arsA	Arsenical pump-driving ATPase	Metal resistance	28	2	NA
arsD	Arsenical resistance operon transacting repressor ArsD	Metal resistance	28	2	NA
tenI	Thiazole tautomerase	Thiamine biosynthesis	22	100	(*9*)
splE	S1B family serine protease SplE	Virulence	15	100	(*10*)
sdrE	Serine-rich repeat-containing protein	Virulence	35	74	(*10*)
mhpC	Arylesterase	Hydrolase	26	60	NA
group_1205	Transcriptional regulator	Transcriptional regulator	81	1	NA
group_4356	Rho termination factor domain-containing protein	Transcriptional regulator	4	59	NA
qacA	Antiseptic resistance protein	Biocide resistance	100	5	NA
qacC	Quaternary ammonium compound-resistance protein QacC	Biocide resistance	35	87	NA
group_2160	Chaperone ATPase	Putative functions	16	84	NA
group_330	Spore coat protein	Putative functions	12	46	NA
bin3_2	Recombinase/resolvase	Mobile genetic element	32	3	NA
group_4660	Putative replication-associated protein	Mobile genetic element	28	1	NA
group_2182	Putative replication-associated protein	Mobile genetic element	54	97	NA
group_3547	IS*1181* transposase	Mobile genetic element	45	78	(*11*)
group_1828	Transposase-associated ATP/GTP binding protein	Mobile genetic element	15	59	(*11*)
group_1679	Transposase for transposon Tn552	Mobile genetic element	2	25	(*11*)
group_278	Recombinase/resolvase	Mobile genetic element	1	20	(*11*)
yueB	Phage infection protein	Phage-related protein	38	85	(*12*)
recT	Putative phage-related DNA recombination protein	Phage-related protein	15	59	(*12*)
group_2472	Phage N-acetlyglucosaminidase	Phage-related protein	15	59	(*12*)
group_2102	Phage protein	Phage-related protein	15	59	NA
group_2856	Phage protein	Phage-related protein	15	59	NA
group_2857	Phage protein	Phage-related protein	15	59	NA
group_3414	Phage protein	Phage-related protein	15	59	NA
group_1521	Phage tape measure protein	Phage-related protein	15	59	NA
group_2854	Putative phage DNA-packaging protein	Phage-related protein	15	59	NA
group_2855	Putative phage head-tail adaptor	Phage-related protein	15	59	NA
group_4784	Putative phage minor structural protein	Phage-related protein	15	59	NA
group_1829	PVL phage protein	Phage-related protein	15	59	NA
group_2103	Phage N-acetlyglucosaminidase	Phage-related protein	15	57	NA
group_2858	Phage tail protein	Phage-related protein	15	56	NA
group_1640	Phage portal protein, SPP1 family	Phage-related protein	15	56	NA
group_3412	Phage terminase, large subunit	Phage-related protein	15	56	NA
group_2860	Phage protein	Phage-related protein	14	56	NA
group_4359	Holin protein	Phage-related protein	14	56	NA
group_3894	Phage minor structural protein GP20	Phage-related protein	14	47	NA
group_3895	Phage minor head protein	Phage-related protein	13	47	NA
group_4788	Phage transcriptional regulator	Phage-related protein	7	46	NA
group_3800	Bacteriophage transcriptional regulator	Phage-related protein	5	24	NA
group_4678	Bacteriophage integrase	Phage-related protein	5	24	NA
group_6539	Bacteriophage terminase small subunit	Phage-related protein	2	43	NA

*Bonferroni $p \leq 0.00002$. Genes encoding hypothetical proteins enriched in lineage G = 55; genes encoding hypothetical proteins enriched in lineage S = 9. NA, not applicable.

Appendix 2 Table 2. List of genes that were exclusively associated with *Staphylococcus saprophyticus* isolates recovered from urinary tract infections*

Gene	Gene predicted function	Biologic function group	% Infection	Reference no.
group_1652	Putative DNA primase-phage associated	Phage-related protein	15	NA
group_2800	Putative phage leukocidin protein	Phage-related protein	8	NA
group_4438	Phage minor structural GP20	Phage-related protein	8	NA
group_1406	Hypothetical protein	Uncharacterized protein	15	NA
group_1405	Hypothetical protein	Uncharacterized protein	15	NA
group_4443	Hypothetical protein	Uncharacterized protein	10	NA
group_3431	Hypothetical protein	Uncharacterized protein	10	NA
group_863	Hypothetical protein	Uncharacterized protein	9	NA
group_4447	Hypothetical protein	Uncharacterized protein	9	NA
group_4446	Hypothetical protein	Uncharacterized protein	9	NA
group_4445	Hypothetical protein	Uncharacterized protein	9	NA
group_4439	Hypothetical protein	Uncharacterized protein	9	NA
group_3617	Hypothetical protein	Uncharacterized protein	7	NA
group_3616	Hypothetical protein	Uncharacterized protein	7	NA
group_1466	Hypothetical protein	Uncharacterized protein	7	NA

*Benjamini Hochberg p≤0.02. NA, not applicable.

Appendix 2 Table 3. List of genes that were enriched in *Staphylococcus saprophyticus* isolates recovered from urinary tract infections*

Gene	Gene predicted function	Biologic function group	% Infection	% Contamination	Reference no.
group_4400	Mph(C) macrolide 2' phosphotransferase	Antimicrobial resistance	25	2	(*13*,*14*)
dfrG	Dihydrofolate reductase	Antimicrobial resistance	9	1	(*14*)
csoR	Copper-sensing transcriptional repressor CsoR	Metal resistance	28	3	NA
cadX	Putative cadmium efflux system accessory protein	Metal resistance	44	13	NA
rep	Plasmid replication initiation protein	Mobile genetic element	18	3	NA
group_2868	Protein rlx	Mobile genetic element	17	2	NA
group_422	Transposase for IS*431mec*	Mobile genetic element	14	2	(*11*)
group_425	Transposase for IS*431mec*	Mobile genetic element	12	2	(*11*)
group_1094	Bacteriophage integrase	Phage-related protein	38	8	(*12*,*14*)
group_4449	DNA packaging protein Staph phage phiRS7	Phage-related protein	19	4	(*12*,*14*)
group_858	Holin protein	Phage-related protein	16	2	(*12*,*14*)
group_1653	Phage protein	Phage-related protein	15	2	(*14*)
group_1392	Phage protein	Phage-related protein	13	2	(*14*)
group_800	Bacteriophage tail tape measure protein	Phage-related protein	13	2	(*14*)
splE	S1B family serine protease SplE	Virulence	55	24	(*10*)
group_3377	Accessory Sec system protein Asp1	Virulence	27	3	(*15*,*16*)
secY_2	Preprotein translocase subunit SecY2	Virulence	27	3	(*15*,*16*)
secA2	Sec family Type I general secretory pathway protein SecA2	Virulence	27	3	(*15*,*16*)
asp3	Accessory Sec system protein Asp3	Virulence	27	3	(*15*,*16*)
asp2	Accessory Sec system protein Asp2	Virulence	27	3	(*15*,*16*)
sraP	Serine-rich repeat-containing protein	Virulence	14	1	(*15*,*16*)
grxC	Glutaredoxin 3	Stress response	30	7	NA
kefF	Glutathione-regulated potassium-efflux system ancillary protein KefF	Stress response	16	3	NA
yhjQ	Putative cysteine-rich protein YhjQ	Stress response	9	1	NA
splE	S1B family serine protease SplE	Virulence	55	24	(*10*)
group_3377	Accessory Sec system protein Asp1	Virulence	27	3	(*15*,*16*)

Gene	Gene predicted function	Biologic function group	% Infection	% Contamination	Reference no.
secY_2	Preprotein translocase subunit SecY2	Virulence	27	3	(*15*,*16*)
secA2	Sec family Type I general secretory pathway protein SecA2	Virulence	27	3	(*15*,*16*)
asp3	Accessory Sec system protein Asp3	Virulence	27	3	(*15*,*16*)
asp2	Accessory Sec system protein Asp2	Virulence	27	3	(*15*,*16*)
sraP	Serine-rich repeat-containing protein	Virulence	14	1	(*15*,*16*)
grxC	Glutaredoxin 3	Stress response	30	7	NA
kefF	Glutathione-regulated potassium-efflux system ancillary protein KefF	Stress response	16	3	NA
yhjQ	Putative cysteine-rich protein YhjQ	Stress response	9	1	NA

*Benjamini Hochberg p≤0.01. Hypothetical proteins (n = 19 genes). NA, not applicable.

Appendix 2 Table 4. List of genes that were exclusively associated with *Staphylococcus saprophyticus* recovered from environmental sources*

Gene	Gene predicted function	Biologic function group	% Contamination	References
group_1467	Hypothetical protein	Uncharacterized protein	42	NA
group_466	Hypothetical protein	Uncharacterized protein	39	NA
group_1991	Hypothetical protein	Uncharacterized protein	32	NA
group_6148	Hypothetical protein	Uncharacterized protein	18	NA
group_6146	Hypothetical protein	Uncharacterized protein	18	NA

*Benjamini Hochberg p≤0.00006. NA, not applicable.

Appendix 2 Table 5. List of genes that were enriched for in *Staphylococcus saprophyticus* isolates recovered from environmental sources*

Gene	Gene predicted function	Biologic function group	% Contamination	% Infection	References
group_227	Type I site-specific deoxyribonuclease restriction subunit	Restriction system	83	32	(*17*)
ccrB	Cassette chromosome recombinase B	Mobile genetic element	61	9	NA
ccrA	Cassette chromosome recombinase A1	Mobile genetic element	54	4	NA
group_1878	Putative replication-associated protein	Mobile genetic element	49	17	NA
group_3001	Myosin-cross reactive antigen (Oleate hydratase)	Stress tolerance	60	6	NA
tetK	Tetracycline resistance protein	Antimicrobial resistance	51	12	(*18*)
cap5O	Capsular polysaccharide biosynthesis protein Cap5O	Capsule	15	1	NA
cap5M	Capsular polysaccharide biosynthesis galactosyltransferase Cap5M	Capsule	13	2	NA
group_1472	Hypothetical protein	Uncharacterized protein	86	56	NA
group_1179	Hypothetical protein	Uncharacterized protein	69	24	NA
group_353	Hypothetical protein	Uncharacterized protein	61	9	NA
group_2224	Hypothetical protein	Uncharacterized protein	59	18	NA
group_1627	Hypothetical protein	Uncharacterized protein	55	25	NA
group_2291	Hypothetical protein	Uncharacterized protein	17	1	NA
group_3863	Hypothetical protein	Uncharacterized protein	10	1	NA

*Benjamini Hochberg p≤0.0001. NA, not applicable.

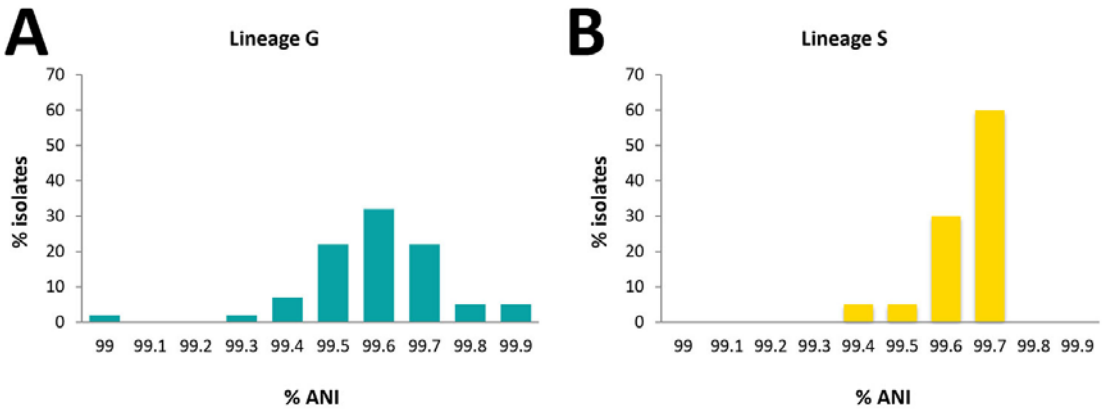

Appendix 2 Figure 1. Measure of genetic diversity between *Staphylococcus saprophyticus* lineage G (A) and lineage S (B) determined by using ANI. Lineage G strains had ANI values of 98.5%–99.999% and appear to be more diverse compared with lineage S strains, which had ANI values of 99.3%–99.991% and were slightly less diverse. Most isolates in lineage G had a lower ANI (99.6%) than the isolates in lineage S (99.7%). The ANI results were comparable to the genetic diversity observed with single nucleotide polymorphism analysis. ANI, average nucleotide identity.

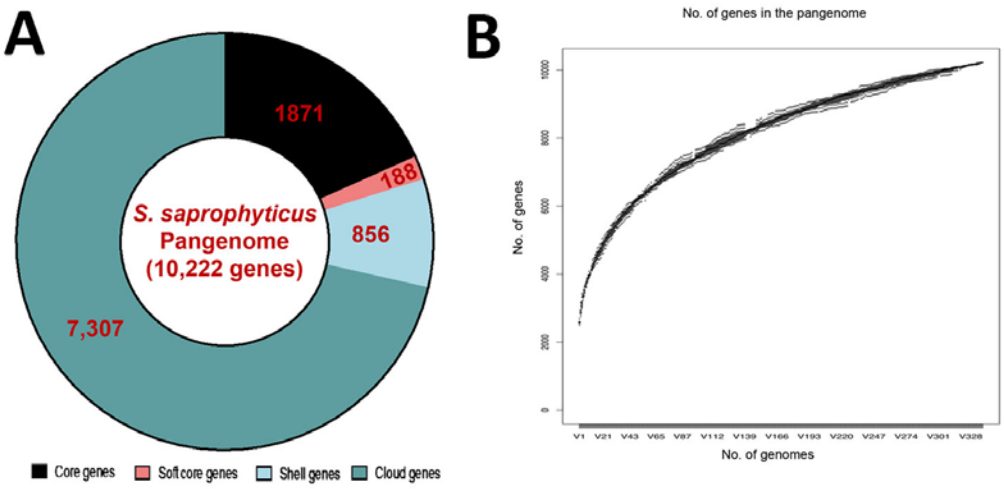

Appendix 2 Figure 2. Pangenome of *Staphylococcus saprophyticus* inferred from 338 isolates recovered from human infections and colonization. Among analyzed isolates, 321 were recovered from UTIs, 12 from blood, 4 from colonization, and 1 from reference strain ATCC 15305 (https://www.atcc.org; GenBank accession no. AP008934.1). A) Distribution of genes in the pangenome generated using Roary (*6*). We found a total of 10,222 genes. The core genes shared by all isolates were constituted of 1,871 genes. We also found 188 soft core genes in 95%–99% of isolates, and 856 shell genes in 15%–94% of isolates. In addition, we noted 7,307 cloud genes <15% of *S. saprophyticus* population. B) Gene accumulation plot for *S. saprophyticus* pangenome as a function of genomes sequenced indicating that *S. saprophyticus* has an open pangenome.

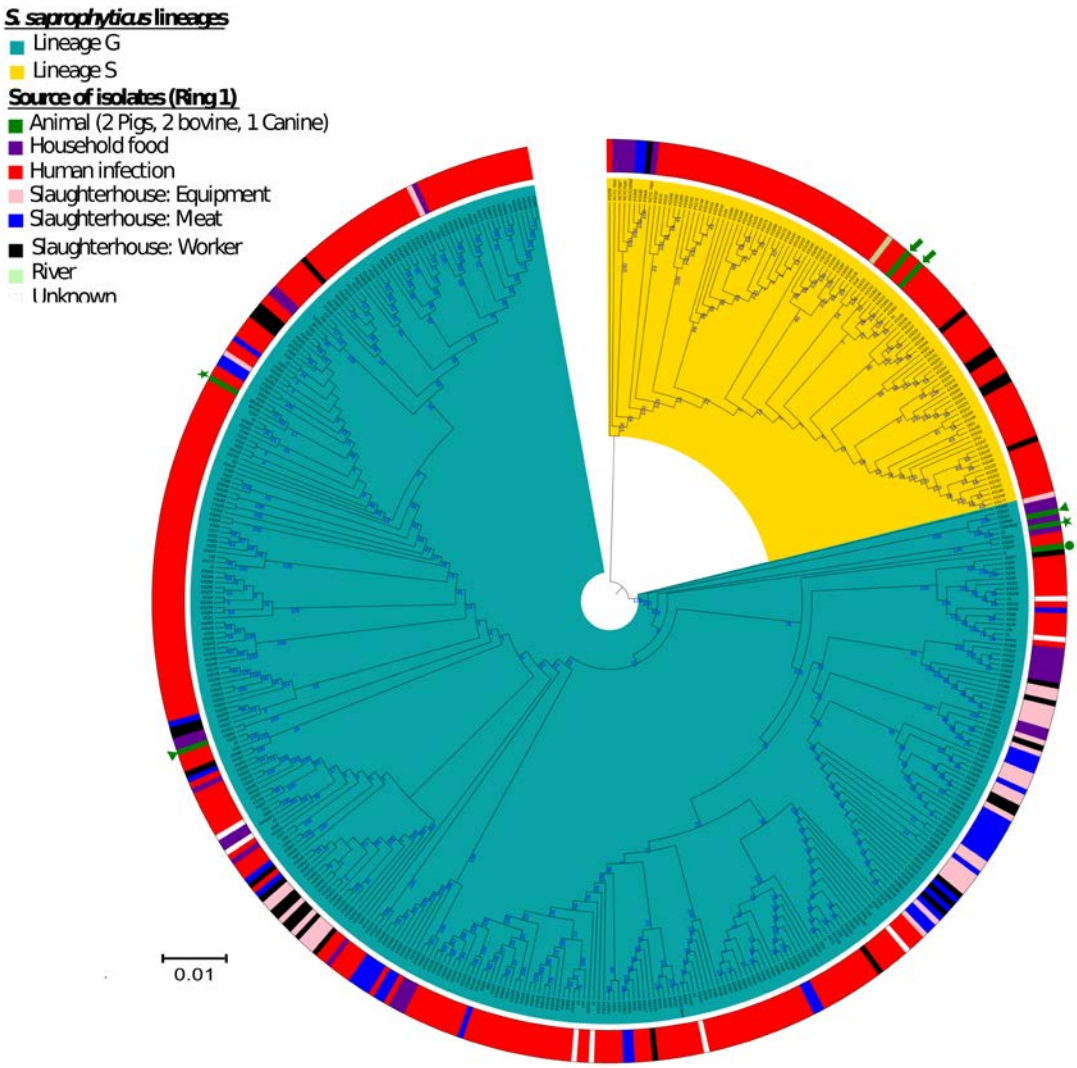

Appendix 2 Figure 3. Single nucleotide polymorphism-based maximum likelihood tree of 480 *Staphylococcus saprophyticus* from different sources. Each node represents a strain. A node with identical color belongs to the same lineage. The assembled contigs were mapped to the reference genome *S. saprophyticus* ATCC 15305 (https://www.atcc.org; GenBank accession no. AP008934.1) and SNPs were called. SNPs generated from each genome were concatenated to single alignment corresponding to position of the reference genome. Polymorphic sites resulting from recombination events in the SNP alignments were filtered out by using Gubbins v2.3.4 (Sanger, https://sanger-pathogens.github.io/gubbins). Maximum likelihood tree was reconstructed using RAxML version 8.2.4 (https://github.com/stamatak/standard-RAxML). The generalized time reversible nucleotide substitution with gamma correction was performed with 100 bootstraps random resampling for support. The image was generated using Interactive Tree of Life (https://itol.embl.de). The colored ring represents the source

of isolates. The green triangles represent strains recovered from pigs, green stars represent strains from bovines, and green circle a strain from a domestic canine. A slaughterhouse isolate recovered from equipment and those from pigs, bovines, and canine were at the base of lineage G, suggesting a probable foodborne origin of this lineage. Conversely, a human infection isolate was at the base of lineage S implying a human origin of this lineage. The green arrows in lineage S depict isolates recovered from small nonhuman primates.

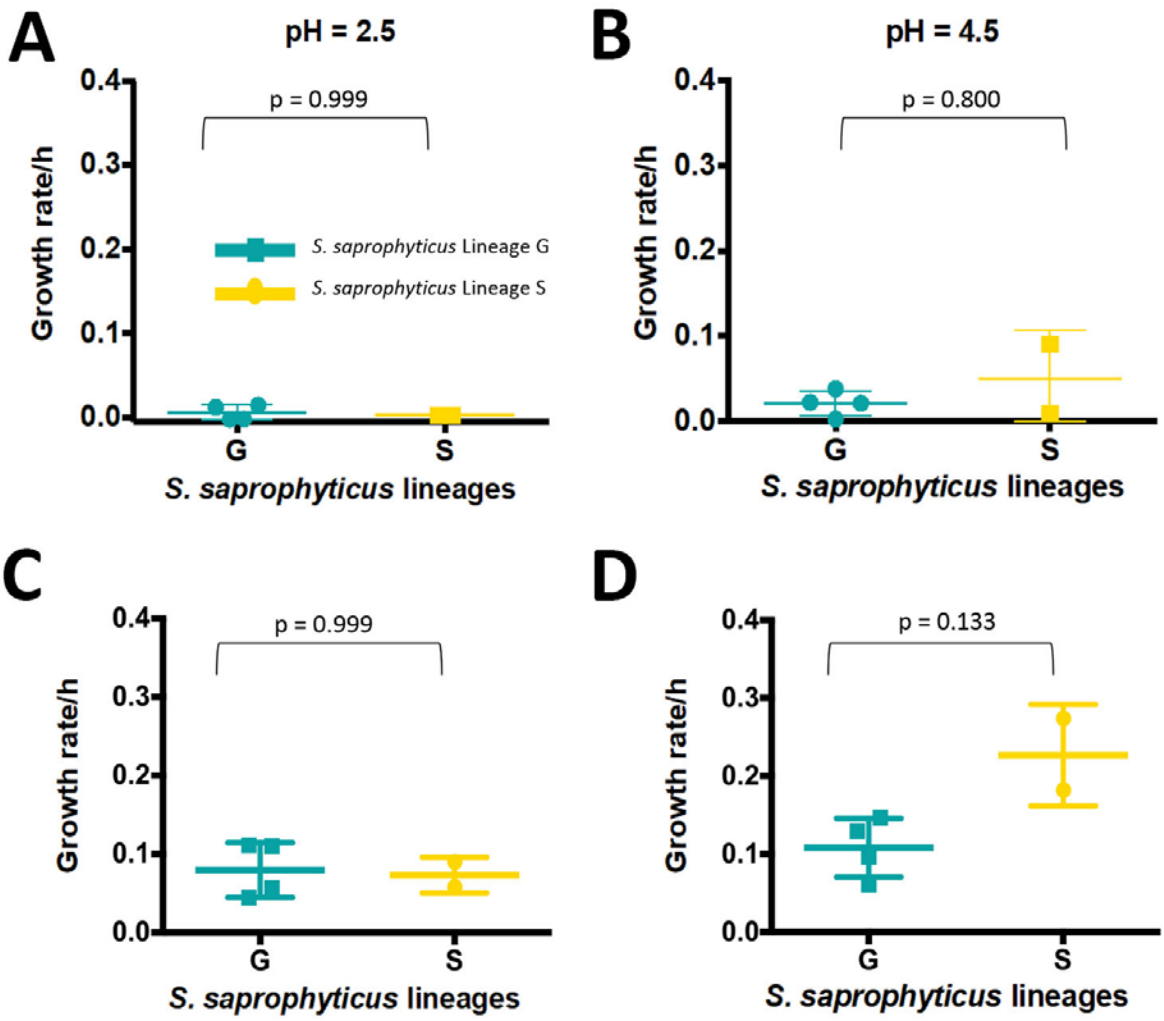

Appendix 2 Figure 4. Growth rate of *Staphylococcus saprophyticus* clonal lineages in different pH levels. A) pH 2.5 representing pH of the human stomach; B) pH 4.5 and C) pH 5.5 representing pH of human skin; and D) pH 8.0 representing pH of urine from a healthy human. Isolates were completely inhibited at pH 2.5 but grew at a low rate when pH = 4.5 and 5.5. The 2 lineages behaved slightly differently in pH = 8.0 but this difference was not statistically significant. Assays were performed in triplicates and each experiment was repeated 3 times. Error bars indicate 95% CI; horizontal lines indicate median.